Journal of Visualized Experiments

Merging Ion Concentration Polarization between Juxtaposed Ion Exchange Membranes for Blocking Propagation of the Polarization Zone

--Manuscript Draft--

Manuscript Number:	JoVE55313R2
Full Title:	Merging Ion Concentration Polarization between Juxtaposed Ion Exchange Membranes for Blocking Propagation of the Polarization Zone
Article Type:	Invited Methods Article - JoVE Produced Video
Keywords:	ion concentration polarization; preconcentration; ion exchange membrane; overlimiting current; electroosmotic flow; electro-osmotic instability
Manuscript Classifications:	10.1.897.520.500.500: Microfluidics; 92.23.1: chemical analysis techniques; 93.34.18: flow visualization (general applications); 93.34.27: fluidics; 93.34.51: mass transfer
Corresponding Author:	Rhokyun Kwak Korea Institute of Science and Technology Seoul, KOREA, REPUBLIC OF
Corresponding Author Secondary Information:	
Corresponding Author E-Mail:	rhokyun@kist.re.kr
Corresponding Author's Institution:	Korea Institute of Science and Technology
Corresponding Author's Secondary Institution:	
First Author:	Minyoung Kim
First Author Secondary Information:	
Other Authors:	Minyoung Kim
	Hyunjoon Rhee
	Ji Yoon Kang
	Tae Song Kim
Order of Authors Secondary Information:	
Abstract:	Ion concentration polarization (ICP) phenomenon is one of the most prevailing methods to preconcentrate low-abundance biological samples. The ICP induces a noninvasive region for charged biomolecules (i.e. ion depletion zone), and we can preconcentrate the targets on this region boundary. Despite the high preconcentration performances with the ICP, it is difficult to find operating conditions of non-propagating ion depletion zones. To overcome this narrow operating window, recently we developed a new platform for spatiotemporally fixed preconcentration. Unlike preceding methods of only using the ion depletion, this platform also utilizes the opposite polarity of the ICP (i.e. ion enrichment) to stop the propagation of the ion depletion zone. By confronting the enrichment zone with the depletion zone, the two zones merge together and stop. In this paper, we describe a detailed experimental protocol to build this spatiotemporally defined ICP platform, and characterize preconcentration dynamics of the new platform by comparing with that of the conventional device. Qualitative ion concentration profiles and current-time responses successfully capture the different dynamics between the merged ICP and the stand-alone ICP. In contrast to the conventional one that can fix the preconcentration location at only ~5V, the new platform can produce a target-condensed plug at a specific location in the broad ranges of operating conditions: voltage (0.5-100 V), ionic strength (1-100 mM), and pH (3.7-10.3).
Author Comments:	Please find the attached cover letter and the response to the editorial review.

Additional Information:	
Question	**Response**
If this article needs to be "in-press" by a certain date, please indicate the date below and explain in your cover letter.	

Korea Institute of
Science and Technology

Rhokyun Kwak, Ph.D
Senior Research Scientist of
Center for BioMicrosystems
rhokyun@kist.re.kr / rhokyun@gmail.com
+82-2-958-6975—Tel
+82-2-958-6910—Fax

To: Jaydev Upponi, Ph.D
Science Editor
JoVE

We are hereby submitting a revised manuscript of our rescent submission titled as "Merging Ion Concentration Polarization between Juxtaposed Ion Exchange Membranes for Blocking Propagation of the Polarization Zone" (Manuscript ID: JoVE55313R1). After the editorial and peer reviews, the article was recommended to add detail experimental protocols and refine the wordings. In this letter, we would like to respectfully request you to consider our revised paper for publication in *the Journal of Visualized Experiments*.

As you and the editors recommended, we clarified the raised issues with detailed explanations and new discussions. In this submission, we provided point-by-point responses to both the editorial and peer review comments individually. I would appreciate your careful consideration of our paper.

With Best Regards,
October 10, 2016

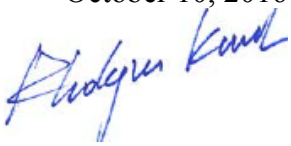

Rhokyun Kwak, Ph.D

TITLE:
Merging Ion Concentration Polarization Between Juxtaposed Ion Exchange Membranes to Block the Propagation of the Polarization Zone

AUTHORS:
Minyoung Kim, Hyunjoon Rhee, Ji Yoon Kang, Tae Song Kim, Rhokyun Kwak

Kim, Minyoung[1,2]
[1]Center for BioMicrosystems
Korea Institute of Science and Technology (KIST)
Seoul, Republic of Korea
[2]Department of Mechanical Engineering,
Seoul National University
Seoul, Republic of Korea
t16012@kist.re.kr

Rhee, Hyunjoon[1,3]
[1]Center for BioMicrosystems
Korea Institute of Science and Technology (KIST)
Seoul, Republic of Korea
[3]Department of Industrial Engineering
University of Illinois Urbana-Champaign, Illinois
hyunjoonrhee@gmail.com

Kang, Ji Yoon[1]
[1]Center for BioMicrosystems
Korea Institute of Science and Technology (KIST)
Seoul, Republic of Korea
jykang@kist.re.kr

Kim, Tae Song[1]
[1]Center for BioMicrosystems
Korea Institute of Science and Technology (KIST)
Seoul, Republic of Korea
tskim@kist.re.kr

Kwak, Rhokyun[1]
[1]Center for BioMicrosystems
Korea Institute of Science and Technology (KIST)
Seoul, Republic of Korea
rhokyun@kist.re.kr

CORRESPONDING AUTHOR:
Kwak, Rhokyun (rhokyun@kist.re.kr; +82-2-958-6975)

KEYWORDS:
ion concentration polarization, preconcentration, ion exchange membrane, overlimiting current, electro-osmotic flow, electro-osmotic instability

SHORT ABSTRACT:
Protocol for a novel ion concentration polarization (ICP) platform that can stop the propagation of the ICP zone, regardless of the operating conditions is described. This unique ability of the platform lies in the use of merging ion depletion and enrichment, which are two polarities of the ICP phenomenon.

LONG ABSTRACT:
Ion concentration polarization (ICP) phenomenon is one of the most prevailing methods to preconcentrate low-abundance biological samples. The ICP induces a noninvasive region for charged biomolecules (*i.e.*, the ion depletion zone), and targets can be preconcentrated on this region boundary. Despite the high preconcentration performances with ICP, it is difficult to find the operating conditions of non-propagating ion depletion zones. To overcome this narrow operating window, we recently developed a new platform for spatiotemporally fixed preconcentration. Unlike preceding methods that only use ion depletion, this platform also uses the opposite polarity of the ICP (*i.e.*, ion enrichment) to stop the propagation of the ion depletion zone. By confronting the enrichment zone with the depletion zone, the two zones merge together and stop. In this paper, we describe a detailed experimental protocol to build this spatiotemporally defined ICP platform and characterize the preconcentration dynamics of the new platform by comparing them with those of the conventional device. Qualitative ion concentration profiles and current-time responses successfully capture the different dynamics between the merged ICP and the stand-alone ICP. In contrast to the conventional one that can fix the preconcentration location at only ~5 V, the new platform can produce a target-condensed plug at a specific location in the broad ranges of operating conditions: voltage (0.5-100 V), ionic strength (1-100 mM), and pH (3.7-10.3).

INTRODUCTION:
Ion concentration polarization (ICP) refers to a phenomenon that occurs during ion enrichment and ion depletion on a permselective membrane, resulting in an additional potential drop with ion concentration gradients[1,2]. This concentration gradient is linear, and it becomes steeper as a higher voltage is applied (Ohmic regime) until the ion concentration on the membrane approaches zero (limiting regime). At this diffusion-limited condition, the gradient (and corresponding ion flux) has been known to be maximized/saturated[1]. Beyond this conventional understanding, when the voltage (or current) is increased further, an overlimiting current is observed, with flat depletion zones and very sharp concentration gradients at the zone boundary[1,3]. The flat zone has a very low ion concentration, but surface conduction, electro-osmotic flow (EOF), and/or electro-osmotic instability promote ion flux and induce an overlimiting current[3-5]. Interestingly, the flat depletion zone serves as an electrostatic barrier, which filters out[6-9] and/or preconcentrates targets[10,11]. Since there is an insufficient amount of ions to screen the surface charges of charged particles (for satisfying electroneutrality), the particles cannot pass through this depletion zone and therefore line up at its boundary. This nonlinear ICP effect is a generic phenomenon in various types of membranes[10-14] and

geometries[6,15-21]; this is why researchers have been able to develop various types of filtration[6-9] and preconcentration[10,11] devices using the nonlinear ICP.

Even with such high flexibility and robustness, it is still a practical challenge to clarify the operating conditions for the nonlinear ICP devices. The nonlinear regime of the ICP quickly removes cations through a cation exchange membrane, which causes the displacement of anions moving towards the anode. As a result, the flat depletion zone propagates quickly, which is reminiscent of shock propagation[22]. Mani *et al.* called this dynamic the deionization (or depletion) shock[23]. To preconcentrate targets at a designated sensing position, preventing the expansion of the ion depletion zone is necessary, for example, by applying EOF or pressure-driven flow against the zone expansion[24]. Zangle *et al.*[22] clarified the criteria for ICP propagation in a one-dimensional model, and it highly depends on electrophoretic mobility[17], ionic strength[18], pH[25], and so on. This indicates that proper operating conditions will be altered according to the sample conditions.

Here, we present detailed design and experimental protocols for a novel ICP platform that preconcentrates targets within a spatiotemporally defined position[26]. The expansion of the ion depletion zone is blocked by the ion enrichment zone, leaving a stationary preconcentration plug at an assigned position, regardless of the operating time, applied voltage, ionic strength, and pH. This detailed video protocol is intended to show the simplest method to integrate cation exchange membranes into microfluidic devices and to demonstrate the preconcentration performance of the new ICP platform compared to the conventional one.

PROTOCOL:

1. Fabrication of Cation Exchange Membrane-Integrated Microfluidic Chips

1.1) Preparation of silicon masters

1.1.1) Design two kinds of silicon masters: one for patterning a cation exchange resin and the other for building a microchannel with polydimethylsiloxane (PDMS).

Note: The detail geometry will be described in the steps 1.3.1 and 1.4.1.

1.1.2) Fabricate the silicon masters by using either conventional photolithography or deep reactive ion etching[27].

1.1.3) Silanize the micropatterned silicon masters with trichlorosilane (~30 μL) in a vacuum jar for 30 min.

CAUTION: Tricholorosilane is a pyrophoric liquid that is flammable and has an acute toxicity (inhalation, oral ingestion).

1.2) Preparation of PDMS molds

1.2.1) Mix a silicone elastomer base with a curing agent at a 10:1 ratio and place the cup with this uncured PDMS (30-40 mL for replicating microstructures on a 4-in silicon wafer) in a vacuum jar for 30 min to remove the bubbles.

Note: The silicone base contains siloxane oligomers terminating with vinyl groups and a platinum-based catalyst. The curing agent contains crosslinking oligomers that have three silicon-hydride bonds[28].

1.2.2) Pour the uncured PDMS on the silicon masters, remove the bubbles with a blower, and cure the PDMS at 80 °C for 2 h in a convection oven.

1.2.3) Detach the cured PDMS from the silicon masters and properly shape the PDMS with a knife (squared shapes, as shown in **Figure 2a-b, iv**).

1.3) Patterning the cation exchange membranes

1.3.1) Cut half of the PDMS mold perpendicularly to the two parallel microchannels and punch holes at the ends of the PDMS channels with a 2.0-mm biopsy punch.

Note: The PDMS mold for patterning the cation selective membrane has two parallel microchannels (width: 100 μm; height: 50 μm; interchannel distance: 100 μm; **Figure 1a**). The original shape of the mold can be imagined by mirroring the sliced mold along the cutting line. L-shaped microchannels are recommended for punching the two holes without overlapping.

1.3.2) Clean a glass slide and the PDMS mold with tape and a blower and put the mold onto the glass slide to create reversible attachment between them.

1.3.3) According to the microflow patterning technique[29], release ~10 μL of a cation exchange resin at the open end of the channel that was sliced in step 1.3.1 (**Figure 1b**). Place the syringe head on the punched holes and pull the plunger (black arrows in **Figure 1b**); a gentle negative pressure will pull the cation exchange resin, and the resin will fill the two channels.

Note: It is recommended that the height of the microchannel is greater than 15 μm, because the high viscosity of the resin requires high pressure to fill the channels. On the other hand, it is better that the height does not exceed 100 μm, because the patterned ion selective membrane will become thicker than 1 μm; such a thick membrane may create a gap between the membrane and the PDMS channel[13].

1.3.4) Detach the PDMS mold without touching the patterned resin and place the glass slide on the heater at 95 °C for 5 min to evaporate the solvent in the resin.

Note: The thickness of the patterned membrane is usually less than < 1 μm. The mold is gently detached by hinging the mold to the open-ended side (dotted line and arrow in **Figure 1b**). It is best to detach the mold less than 1 min after filling the resin. If the mold is detached a few minutes later, thicker membranes could be obtained, but they would have a concave shape due to the capillary effect.

1.3.5) Peel off the unnecessary part of the patterned membrane with a razor blade, making two separated line-patterns (**Figure 1c**).

Note: The cation exchange material used here has perfluorinated groups, meaning the pattern is not strongly bonded to the glass. Therefore, the simple blading method can easily remove the unnecessary part of the membrane.

1.4) Integration of the microchannel and the membrane-patterned substrate

1.4.1) Punch two holes at the ends of microchannels and another two holes where the membrane patterns will be located after bonding the PDMS channel to the membrane-patterned substrate fabricated in step 1.3.

Note: The PDMS microchannel has one channel (width: 50-100 μm; height: 10 μm), but it is bonded to the ends of the neighboring channel (**Figure 1d**).

1.4.2) Bond the PDMS microchannel to the membrane-patterned substrate immediately after oxygen plasma treatment for 40 s at 100 W and 50 mTorr.

Note: Place the patterned membrane perpendicularly on the middle of the microchannel.

2. ICP Preconcentration

2.1) Preparation for the experiment

2.1.1) Prepare various test solutions, including 1-100 mM KCl, 1 mM NaCl (pH ~7), the mixture of 1 mM NaCl and 0.2 mM HCl (pH ~3.7), the mixture of 1 mM NaCl and 0.2 mM NaOH (pH ~10.3), and 1X phosphate-buffered saline.

2.1.2) Add a negatively charged fluorescent dye (~1.55 μM) to the test solutions.

Note: The concentration of the added dye should be much lower than that of the salt ions (< 10 μM) so that the charged dyes do not contribute to an electrical current[30,31].

2.1.3) Load the sample solution in one reservoir of the channel and apply negative pressure to the other reservoir to fill the channel with the solution. Connect the two reservoirs hydrodynamically by releasing a large droplet to eliminate the pressure gradient along the channel (**Figure 2a**).

2.1.4) Fill the two reservoirs, which are connected to the cation exchange patterns, with buffer solutions (1 M KCl or 1 M NaCl) using a syringe or a pipet to compensate for the ICP effect in the reservoirs.

2.1.5) Place the wires at the reservoirs, across the two patterned membranes (anode on the left reservoir and cathode on the right), and connect them with a source measurement unit (**Figure 2a**).

2.2) Visualization of the ICP phenomenon and ICP preconcentration

2.2.1) Load the ICP device on an inverted epifluorescence microscope. Apply a voltage (0.5-100 V) and measure the current response with a source measurement unit.

2.2.2) Capture fluorescent images with a charge-coupled device camera and analyze the fluorescent intensity using imaging software[32].

REPRESENTATIVE RESULTS:

The schematic fabrication steps of a membrane-integrated microfluidic preconcentrator are shown in **Figure 1**. A detailed description of the fabrication is given in the Protocol. The designs

and device images of the spatiotemporally defined preconcentrator[26] are contrasted with those of a conventional preconcentrator[11] (**Figure 2)**. The ICP phenomenon in the spatiotemporally defined preconcentrator was investigated in terms of current-voltage-time responses and fluorescent intensity profiles (**Figure 3-4)**. Similar to the ICP phenomenon with a single-membrane preconcentrator[3,11], three different regimes (Ohmic, limiting, and overlimiting) were observed in the current-voltage curve: 0.5-1 V (Ohmic and limiting) and 5 V (overlimiting). However, a nonconventional current recovery was detected in the current-time curve as the ion enrichment and the ion depletion zones merged. Next, the ICP preconcentration was tested at different times and voltages with the spatiotemporally defined preconcentrator (**Figure 5**) and the conventional one-membrane device (**Figure 6**). The preconcentration dynamics were quantified by fluorescence images, current-time responses, and fluorescent intensity graphs over different distances and times. When comparing the two platforms, the new ICP platform shows an advantage in always collecting targets (fluorescent dyes) between the two cation selective membrane patterns. In addition, it was confirmed that the preconcentration plug remains the same in different ionic strengths (1-100 mM NaCl) and pH values (3.7-10.3), verifying the high availability of the merging ICP preconcentrator in wide ranges of operating conditions (**Figure 7**). In **Figure 8**, a 10,000-fold protein preconcentration was also demonstrated.

FIGURE LEGENDS:

Figure 1. Fabrication steps of a cation exchange membrane-integrated microfluidic chip. After a PDMS mold is filled with a cation exchange resin using the microflow patterning technique (a-c)[29], the membrane-patterned glass substrate is bonded with a PDMS microchannel by oxygen plasma treatment (d).

Figure 2. **Schematics of the spatiotemporally defined preconcentrator (a) and conventional preconcentrator (b).** (a) In the new platform, between two membrane patterns (i), ion depletion/enrichment zones are developed and merged together with linear (Ohmic and limiting regime; ii) or nonlinear (overlimiting regime; iii) concentration profiles. In all three current regimes, the ion enrichment zone blocks the propagation of the depletion zone and targets (hollow circles; i) are preconcentrated at the interface of the ion depletion and enrichment zones (curved, dotted line; i). The wall of the PDMS channel is negatively charged, and this generates electro-osmotic flow (EOF) between the two cation exchange membranes under an electric field. The EOF continuously delivers targets towards the interface of the depletion and enrichment zones. (b) In the conventional platform, only the ion depletion zone is developed near the membrane with linear (Ohmic and limiting regime; ii) and nonlinear (overlimiting regime; iii) concentration gradients. As the EOF delivers the targets, the preconcentation also occurs at the depletion zone boundary, but this zone (and the preconcentrated plug) moves away from the cation exchange membrane (black arrow; i). It is noted that there is no increase in the ion concentration here without the ion enrichment zone (ii-iii). In (a-b), the device images are shown in (iv). C_0 represents the initial ion concentration. V^+ and G indicate the anode and the cathode, respectively. Reprinted from Reference 26t with permission from The American Chemical Society.

Figure 3. Merged ICP phenomenon between two cation exchange membranes. (a) The current-voltage curve shows three distinct regimes (Ohmic, limiting, and overlimiting). The current response is measured by ramping up the voltage at discrete intervals of 0.25 V every

40 s, which is repeated three times. The error bar indicates the standard deviation of the current responses. (b, c) In the three regimes, fluorescence images (b) and intensity profiles along A-A′ at the middle of the channel (c) were obtained. Yellow, dotted boxes indicate the locations of the cation selective membranes. 1 mM KCl solution with a 1.55 μM (1 μg/mL) negatively charged fluorescent dye was used. Reprinted from Reference 26 with permission from The American Chemical Society.

Figure 4. Transient dynamics of merging ion depletion and enrichment zones. (a, b) In the Ohmic-limiting regimes, the linear concentration gradients grow (< 1 s) from the cation exchange membrane and then overlap together (> 1 s). (c) In the overlimiting regime, the two ICP zones are merged more quickly (< 0.6 s) with the depletion shock (black arrow at 0.2 s). (d-f) The current-time responses show that the current is initially dropped due to the growth of the low-concentration depletion zone, which corresponds to low electrical conductivity. The current drop is then recovered due to a convective transport by vortices confined between two membranes. Reprinted from Referenced 26 with permission from The American Chemical Society.

Figure 5. Spatiotemporally fixed preconcentration at 5, 10, and 20 V. (a-c) Fluorescence images of the merged ICP and the current-time responses (d-f) over time (0-100 s). The yellow, dotted lines indicate the location of the cation exchange membranes. (g) Time-lapse fluorescent intensity profiles are plotted along the microchannel (A-A′). The peak intensities increase as time passes, with fixed locations. (h) The peak intensity fold (*i.e.*, how many times greater than the initial fluorescent intensity). At higher voltages, the faster EOF delivers targets towards the interface of the ion depletion and enrichment zones, so the preconcentration speed increases. A spike at 20 V is induced by the depletion shock (Figure 4c). The fluorescent dyes accumulate on the shock boundary as it pushes the dyes. This initial accumulation is then somewhat dispersed when the depletion shock meets the ion enrichment zone, creating the spike in the peak intensity curve. As can be seen in Figure 4c, at 0.8 s, the peak was wider than it was at 0.4 s. This is probably because the left side of the left Nafion pattern (Figure 2a) was electrically floated, and the accumulated dyes could spread out. Reprinted from Reference 26 with permission from The American Chemical Society.

Figure 6. ICP phenomenon in the conventional ICP preconcentrator at 5, 10, and 20 V. (a-c) Fluorescence images of the ion depletion zone and the current-time response (d-f) over time (0-100 s). The propagation of the depletion zone and the preconcentration plug is clearly visualized in the fluorescence images. Accordingly, the vortices are not confined, so the current recovery does not occur, even in the overlimiting regime. Yellow, dotted lines mark the location of the cation exchange membranes. (g) Time-lapse fluorescent intensity profiles are plotted along the microchannel (A-A′). The peak intensities increase as time passes, but the location moves away from the membrane. (h) Peak intensity fold of the conventional ICP device. In contrast to the merged ICP device (Figure 5h), there is no intensity spike without the confinement of ICP zones, because the fluorescent intensity increased as the dye was preconcentrated. The increase of the peak intensity fold is similar to that of the merged ICP device at the same time (at a given voltage). This indicates that the length of time that the preconcentrated plug is held in place is crucial to the preconcentration performance.

Figure 7. Spatiotemporally defined preconcentration at various ionic strengths (1-100 mM NaCl) and pH values (3.7-10.3). (a) Fluorescence images obtained after 100 s of operation at 50 V. As can be seen, the locations of the preconcentration plugs are still between the two cation exchange membranes (yellow, dotted lines), even though the intensity is weakened under high ionic strength and in a strong acidic or basic solution. (b, c) The location of the peak intensity and its intensity fold (*i.e.*, how many times greater than the initial intensity), mapped under 10, 20, 50, and 100 V. For a single condition (1, 10, 100 mM and/or pH 3.7, 7, and 10), there are four data points corresponding to the four voltage conditions. At higher voltages, there is a higher peak intensify fold in all cases. 100 V was not tested in 1 mM NaCl (pH 7) because the peak intensity already touched the highest values (due to the saturation of the camera) at 50 V. From the peak intensity profile, the peak region is also identified, with 1% below the peak intensity, which is represented by error bars (b, c). A higher voltage and a stronger EOF shift the peak location to the right, with a higher intensity fold and a sharper preconcentration plug. Gray boxes indicate the locations of the cation exchange membranes. The 0 distance (a) represents the origin of the x-axis (b, c), which is on the right edge of the left cation exchange membrane. The origin of the distance is the right edge of the left membrane. Reprinted from Reference 26 with permission from The American Chemical Society.

Figure 8. Demonstration of spatiotemporally fixed protein preconcentration. FITC-albumin (1 μg/mL) in 1X phosphate-buffered saline solution was used. 0.1% Tween 20 was also added to prevent nonspecific binding. Since the preconcentration is hardly achieved at a higher ionic strength (Figure 7), we doubled the width of the Nafion pattern (200 μm) and used a narrower PDMS channel (50 μm). In this way, the performance of ICP preconcentration was enhanced by broadening the ion pathway and reducing the absolute amount of ions in the channel. At an applied voltage of 100 V, the peak and averaged fluorescent intensities were traced in the white, dotted box, which is the region between the two cation exchange membranes. Within 10 min of operation, the proteins were preconcentrated up to 10 mg/mL (peak) and ~0.1 mg/mL (averaged), indicating 10,000- and 100-fold preconcentrations, respectively. The inset fluorescence images were obtained at 0, 10, and 20 min. In this work, a 20-min operation was enough to preconcentrate the target molecules, so we did not cover longer operating times. Reprinted from Reference 26 with permission from The American Chemical Society.

DISCUSSION:

We have described the fabrication protocol and the performance of a spatiotemporally defined preconcentrator in a range of the applied voltage (0.5-100 V), ionic strength (1-100 mM), and pH (3.7-10.3), achieving a 10,000-fold preconcentration of dyes and protein within 10 min. As like previous ICP devices, the preconcentration performance becomes better at higher voltage and at lower ionic strength. One additional parameter we can consider here is the distance between two cation exchange membranes. If we increase the inter-membrane distance, the electric field decreases under the same applied voltage, resulting in the decrease of the preconcentration speed[26].

The microflow patterning technique[29] used in this work is a robust method for patterning cation exchange resins, so it has been one of the gold-standard methods for integrating the ion exchange materials into microfluidic systems. Nevertheless, it is necessary to to fabricate two juxtaposed cation exchange membranes with a short intermembrane distance (smaller than few hundred

micrometers). In steps 1.3.3-1.3.4, the cation exchange resin is in a liquid phase. Therefore, the resin in the two microchannels can be collapsed, and the remaining resin drop at the open end of the channels can also flood during the mold detachment (step 1.3.4.). To build two cation exchange membranes with high pattern fidelity, we used the resin with a relatively high viscosity (20% of the cation exchange material in the solvents) and carefully set the detachment process with a designated detaching direction.

Even though the high operating flexibility of this platform was demonstrated, the reader might be concerned about determining the optimal conditions from the wide range within the operating window. One representative trade-off is between the preconcentration speed and the stability of the ICP effect. As can be seen in Figure 5 in Kwak *et al.*[26], a high applied voltage (> 50 V) can condense targets quickly; however, this also induces strong vortices in the depletion zone (1 mM / pH 7 in Figure 7a), which decreases the stability of the sample preconcentration. Accordingly, the preconcentration speed becomes difficult to predict[33]. In the current stage, we recommend experimental conditions with a relatively low voltage (< 30 V) and ionic strength (< 10 mM) for a stable, predictable, and spatiotemporally fixed preconcentration. This trade-off between the preconcentration speed and the stability of the preconcentrated plug is also related to the sources of the nonlinear ICP (surface conduction, EOF, and electro-osmotic instability). The main source of the nonlinear ICP at a relatively small voltage (< 50 V) is EOF, creating a coherent vortex pair in the depletion zone (**Figure 3b**), which leads to a stable preconcentration. At a relatively high voltage (> 50 V), the main source of the nonlinear ICP is changed to electro-osmotic instability, resulting chaotic multiple vortexes, which decrease the stability of the preconcentration.

Recently, paper-based ICP platforms have been developed by Phan *et al.*[34], Gong *et al.*[19], and Han *et al*[21]. These paper devices with microporous structures can suppress electro-osmotic instability[4,35] and alleviate the stability issue. However, the sizes of the paper channels are generally about 0.5-5 mm, which is much bigger than a conventional microfluidic channel. This wider paper channel with random fiber networks causes irregular motions in the preconcentrated plugs. This has been inevitable in paper-based ICP preconcentrators, because the minimum feature size of wax patterning and paper cutting (*i.e.*, fabrication methods to build paper channels) is about few hundred micrometers.

The ICP preconcentrator has been used in a wide range of biomicrofluidic platforms for preconcentrating various bio-agents; amplifying the signals of various assays; and detecting targets, such as therapeutic proteins[36], peptides[37], aptamers[17], and enzymes[38]. These previous works targeted fluorescence-labeled biomolecules. This is because we cannot specify the exact operating conditions *(i.e.*, voltage and flow rate) to maintain the preconcentration site, so we first need to find the proper conditions for the preconcentrator targets. Departing from previous work, the merged ICP phenomenon allows us to always fix the preconcentrated plugs at a broad range of operating conditions while maintaining the high flexibility of the ICP devices. This indicates that we can now extend the applications of ICP preconcentrators to label-free detection techniques without using visualization instruments and tracers. This unique advantage of the spatiotemporal controllability provides a strong commercial opportunity to integrate the ICP device with generic benchtop platforms, such as polymerase chain reaction machines and mass spectrometers.

ACKNOWLEDGEMENTS:
This work was supported by the internal fund of the Korea Institute of Science and Technology (2E26180) and by the Next Generation Biomedical Device Platform program, funded by the National Research Foundation of Korea (NRF-2015M3A9E202888).

DISCLOSURE:
The authors have nothing to disclose.

REFERENCES:
1. Probstein, R. F. *Physicochemical Hydrodynamics: An Introduction, 2nd ed*. Wiley-Interscience. New York (2003).
2. Strathmann, H. *Ion-Exchange Membrane Separation Processes*. Elsevier. Amsterdam (2004).
3. Dydek, E.V., *et al.* Overlimiting Current in a Microchannel. *Phys. Rev. Lett.* **107** (11), 118301, doi:10.1103/PhysRevLett.107.118301 (2011).
4. Kwak, R., Pham, V.S., Lim, K.M., & Han, J.Y. Shear flow of an electrically charged fluid by ion concentration polarization: scaling laws for electroconvective vortices. *Phys. Rev. Lett.* **110** (11), 114501, doi:10.1103/PhysRevLett.110.114501 (2013).
5. Rubinstein, I., & B. Zaltzman, B. Electro-osmotically induced convection at a permselective membrane. *Phys. Rev. E* **62** (2), 2238-2251, doi:10.1103/PhysRevE.62.2238 (2000).
6. Kwak, R., Kim, S., & Han, J. Continuous-flow biomolecule and cell concentrator by ion concentration polarization. *Anal. Chem.* **83** (19), 7348-7355, doi:10.1021/ac2012619 (2011).
7. Jeon, H., Lee, H., Kang, K.H., & Lim, G. Ion concentration polarization-based continuous separation device using electrical repulsion in the depletion region. *Sci. Rep.* **3**, 3483, doi:10.1038/srep03483 (2013).
8. Kim, S.J., Ko, S.H., Kang K.H., & Han, J. Direct seawater desalination by ion concentration polarization. *Nat. Nanotechnol.* **5** (4), 297-301, doi:10.1038/nnano.2010.34 (2010).
9. MacDonald, B.D., Gong, M.M., Zhang, P., & Sinton, D. Out-of-plane ion concentration polarizationfor scalable water desalination. *Lab Chip* **14** (4), 681-685, doi:10.1039/C3LC51255J (2014).
10. Schoch, R.B., Han, J.Y., & Renaud, P. Transport phenomena in nanofluidics. *Rev. Mod. Phys.* **80** (3), 839-883, doi:10.1103/RevModPhys.80.839 (2008).
11. Kim, S.J., Song, Y.A., & Han, J. Nanofluidic concentration devices for biomolecules utilizing ion concentration polarization: theory, fabrication, and applications. *Chem. Soc. Rev*. **39** (3), 912-922, doi:10.1039/b822556g (2010).
12. Mai, J.Y., Miller, H., & Hatch, A.V. Spatiotemporal mapping of concentration polarization Induced pH changes at nanoconstrictions. *ACS Nano* **6** (11), 10206-10215, doi:10.1021/nn304005p (2012).
13. Kim, B., *et al.* Tunable ionic transport for a triangular nanochannel in a polymeric nanofludic system. *ACS Nano* **7** (1), 740-747, doi:10.1021/nn3050424 (2013).
14. Syed, A. Mangano, L. Mao, P.Han J., & Song, Y.-A. Creating sub-50 nm nanofluidic junctions in a PDMS microchip via self-assembly process of colloidal silica beads for

electrokinetic concentration of biomolecules. *Lab Chip* **14**, 4455-4460, doi:10.1039/C4LC00895B (2014).
15. Wang Y.C., Stevens, A.L., & Han, J.Y., Million-fold preconcentration of proteins and peptides by nanofluidic filter. *Anal. Chem.* **77** (14), 4293-4299, doi:10.1021/ac050321z (2005).
16. Lee, J.H., Cosgrove, B.D., Lauffenburger, D.A., & Han, J. Microfludic concentration-enhanced cellular kinase activity assay. *J. Am. Chem. Soc.* **131** (30), 10340-10341, doi:10.1021/ja902594f (2009).
17. Cheow, L.F. & Han, J.Y. Continuous signal enhancement for sensitive aptamer affinity probe electrophoresis assay using electrokinetic concentration. *Anal. Chem.* **83** (18), 7086-7093, doi:10.1021/ac201307d (2011).
18. Ko, S.H., *et al.* Nanofluidic preconcentration device in a straight microchannel using ion concentration polarization. *Lab Chip* **12** (21), 4472-4482, doi:10.1039/C2LC21238B (2012).
19. Gong, M.M., Nosrati, R., Gabriel, M.C.S., Zini, M., & Sinton, D. Direct DNA analysis with paper-based ion concentration polarization. *J. Am. Chem. Soc.* **137** (43), 13913–13919, doi:10.1021/jacs.5b08523 (2015).
20. Hong, S., Kwak, R., & Kim, W. Paper-based flow fractionation system applicable to preconcentration and field-flow separation. *Anal. Chem.* **88** (3), 1682–1687, doi:10.1021/acs.analchem.5b03682 (2016).
21. Han, S.I., Hwang, K.S., Kwak, R., & Lee, J.H. Microfluidic paper-based biomolecule preconcentrator based on ion concentration polarization. *Lab Chip* **16**, 2219-2227, doi:10.1039/C6LC00499G (2016).
22. Zangle, T.A., Mani, A., & Santiago, J.G. Theory and experiments of concentration polarization and ion focusing at microchannel and nanochannel interfaces. *Chem. Soc. Rev.* **39** (3), 1014-1035, doi:10.1039/B902074H (2010).
23. Mani, A., & Bazant, M.Z. Deionization shocks in microstructures. *Phys. Rev. E* **84**, 061504, doi:10.1103/PhysRevE.84.061504 (2011).
24. Slouka, Z., Senapati, S., & Chang, H.C. Microfluidic systems with ion-selective membranes. *Annu. Rev. Anal. Chem.* **7**, 317-335, doi:10.1146/annurev-anchem-071213-020155 (2014).
25. Kirby, B.J., & Hasselbrink, E.F. Zeta potential of microfluidic substrates: 1. Theory, experimental techniques, and effects on separations. *Electrophoresis* **25** (2), 187-202, doi:10.1002/elps.200305754 (2004).
26. Kwak, R., Kang, J.Y., & Kim, T.S. Spatiotemporally defining biomolecule preconcentration by merging ion concentration polarization. *Anal. Chem.* **88** (1), 988−996, doi:10.1021/acs.analchem.5b03855 (2016).
27. Duffy, D.C., McDonald, J.C., Schueller, O.J.A., & Whitesides, G.M. Rapid prototyping of microfluidic systems in poly(dimethylsiloxane). *Anal. Chem.* **70** (23), 4974-4984, doi:10.1021/ac980656z (1998).
28. Campbell, D.J., *et al*. Replication and compression of surface structures with polydimethylsiloxane elastomer. *J. Chem. Educ.* **76**(4), 537-541, doi:10.1021/ed076p537 (1999).
29. Lee, J.H., Song, Y.A., & Han, J.Y. Multiplexed proteomic sample preconcentration device using surface-patterned ion-selective membrane. *Lab Chip* **8** (4), 596-601, doi:10.1039/b717900f (2008).

30. Kwak, R., Guan, G., Peng, W.K., & Han, J. Microscale electrodialysis: concentration profiling and vortex visualization. *Desalination* **308**, 138–146, doi:10.1016/j.desal.2012.07.017 (2013).
31. Chambers, R.D. & Santiago, J.G. Imaging and quantification of isotachophoresis zones using nonfocusing fluorescent tracers. *Anal. Chem.* **81**, 3022–3028, doi:10.1021/ac802698a (2009).
32. Rasband, W.S., ImageJ, U. S. National Institutes of Health, Bethesda, Maryland, USA, http://imagej.nih.gov/ij/, 1997-2016 (2016).
33. Minerick, A.R., Ostafin, A.E., & Chang, H.C. Electrokinetic transport of red blood cells in microcapillaries. *Electrophoresis* **23** (14), 2165-2173, doi:10.1002/1522-2683(200207)23:14<2165::AID-ELPS2165>3.0.CO;2-# (2002).
34. Phan, D-.T., Shaegh, S.A.M, Yang, C., & Nguyen, N-.T. Sample concentration in a microfluidic paper-based analytical device using ion concentration polarization. *Sens. Actuators B* **222**, 735-740 doi: 10.1016/j.snb.2015.08.127 (2016).
35. Rubinstein, S.M., Direct observation of a nonequilibrium electro-osmotic instability. *Phys. Rev. Lett.* **101**, 236101 doi: 10.1103/PhysRevLett.101.236101 (2008).
36. Ouyang, W., *et al.* Microfluidic platform for assessment of therapeutic proteins using molecular charge modulation enhanced electrokinetic concentration assays. *Anal. Chem.* **88**, 9669-9677, doi:10.1021/acs.analchem.6b02517 (2016).
37. Cheow, L.F., Sarkar, A., Kolitz, S., Lauffenburger, D., & Han, J. Detecting kinase activities from single cell lysate using concentration-enhanced mobility shift assay. *Anal. Chem.* **86**, 7455-7462, doi:10.1021/ac502185v (2014).
38. Chen, C-.H., *et al*., Enhancing protease activity assay in droplet-based microfluidics using a biomolecule concentrator. *J. Am. Chem. Soc.* **133**, 10368-10371, doi:10.1021/ja2036628 (2011).

Figure1

Click here to download Figure Figure1.pdf

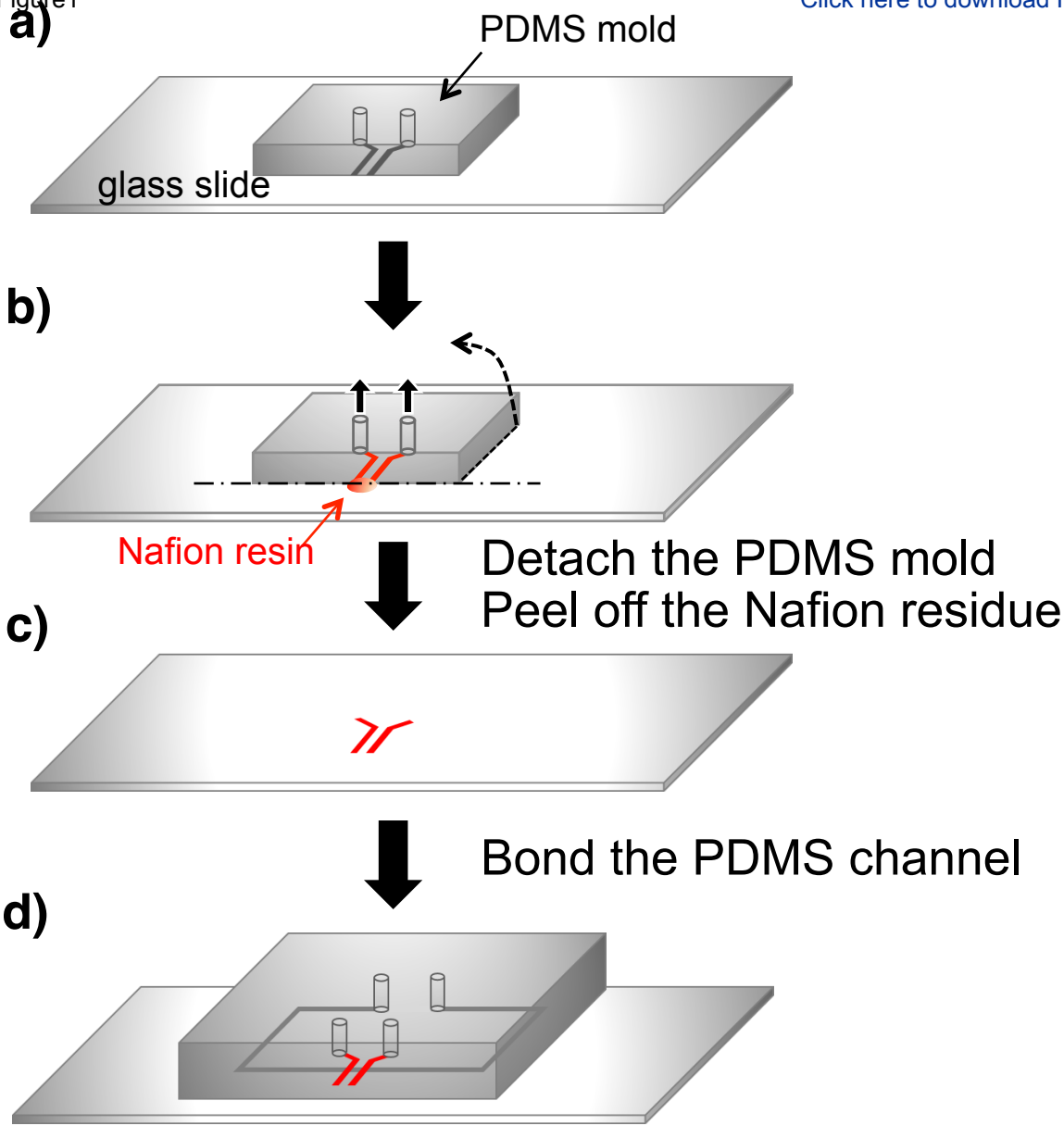

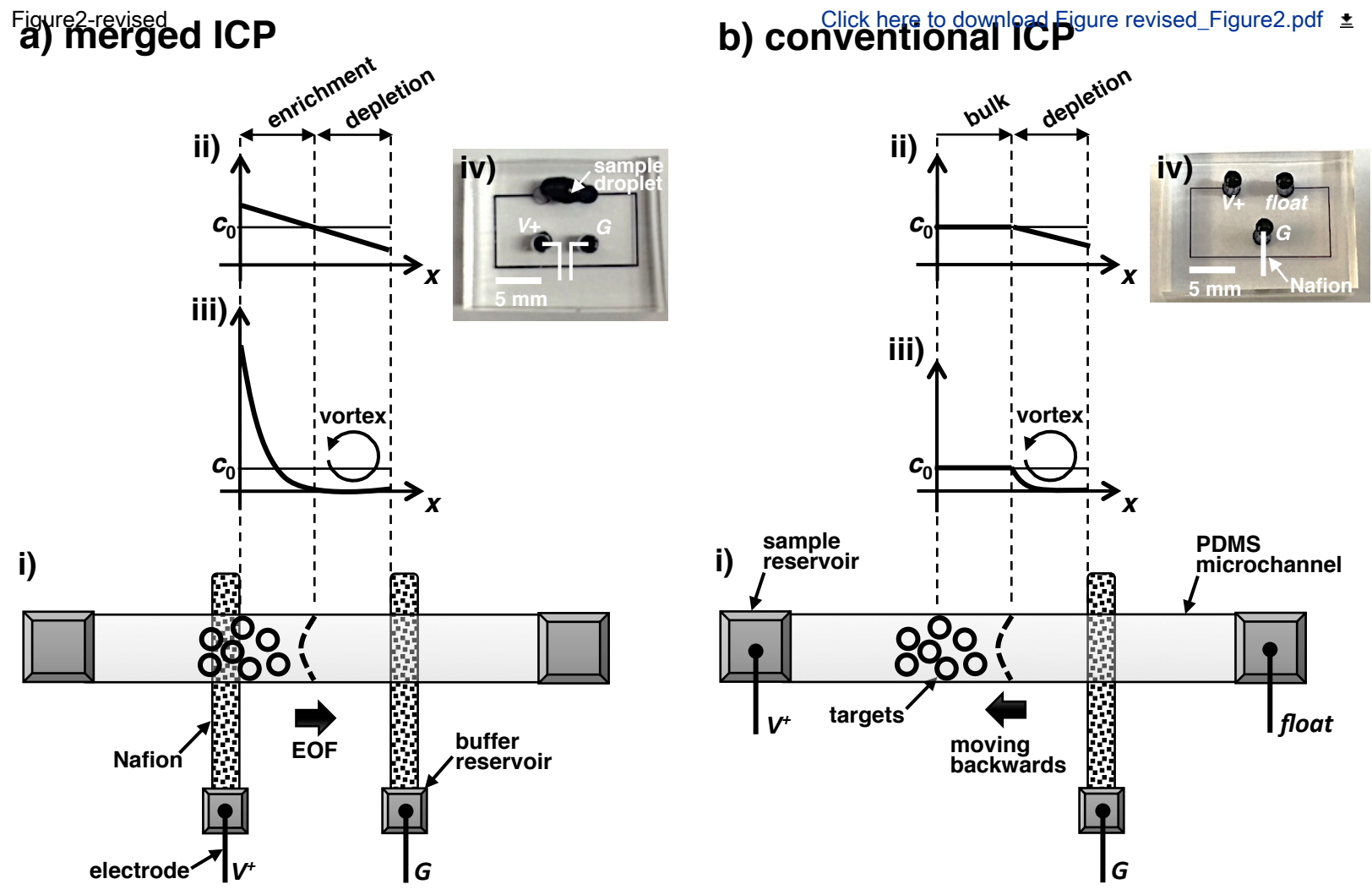

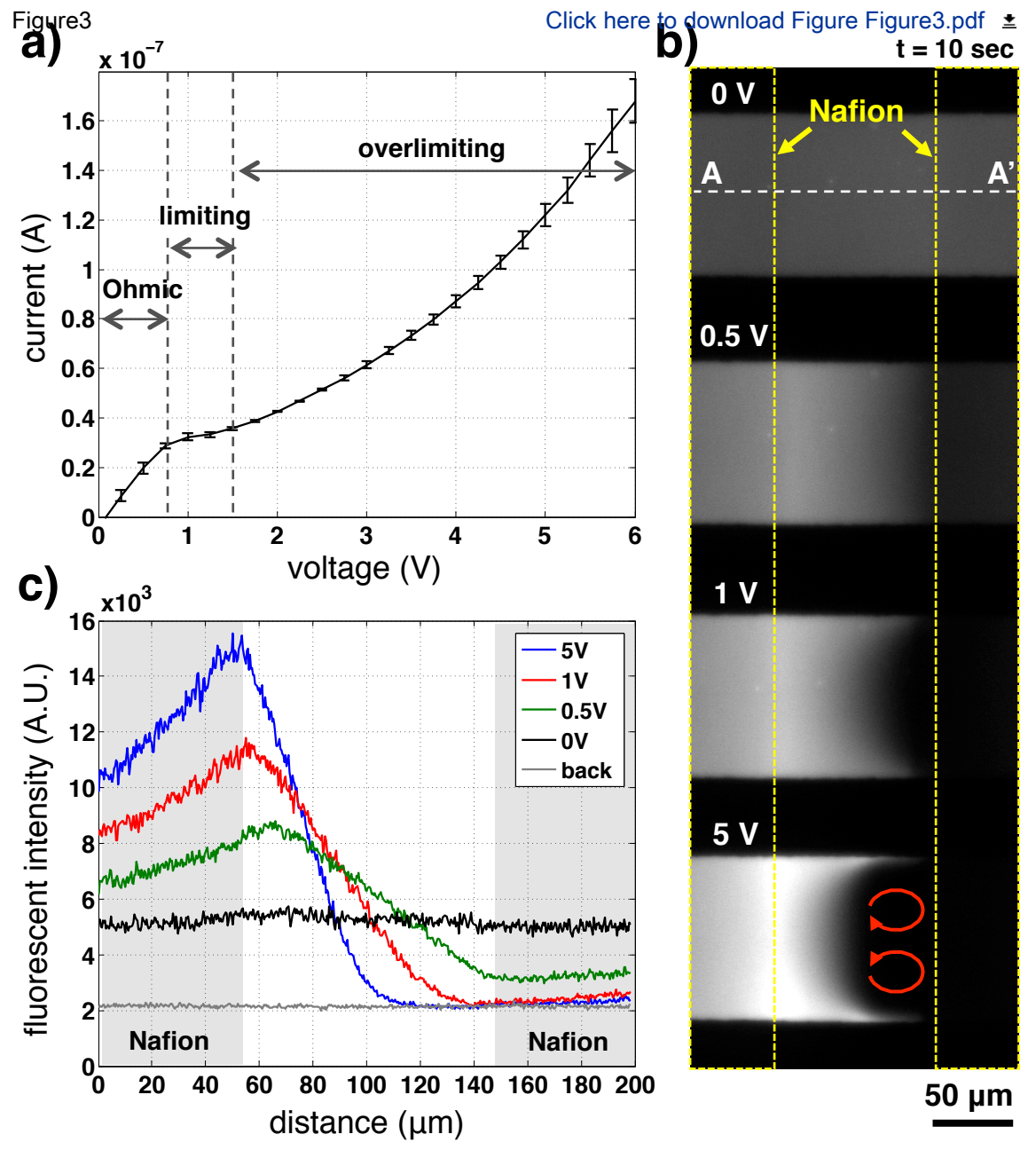

Figure4

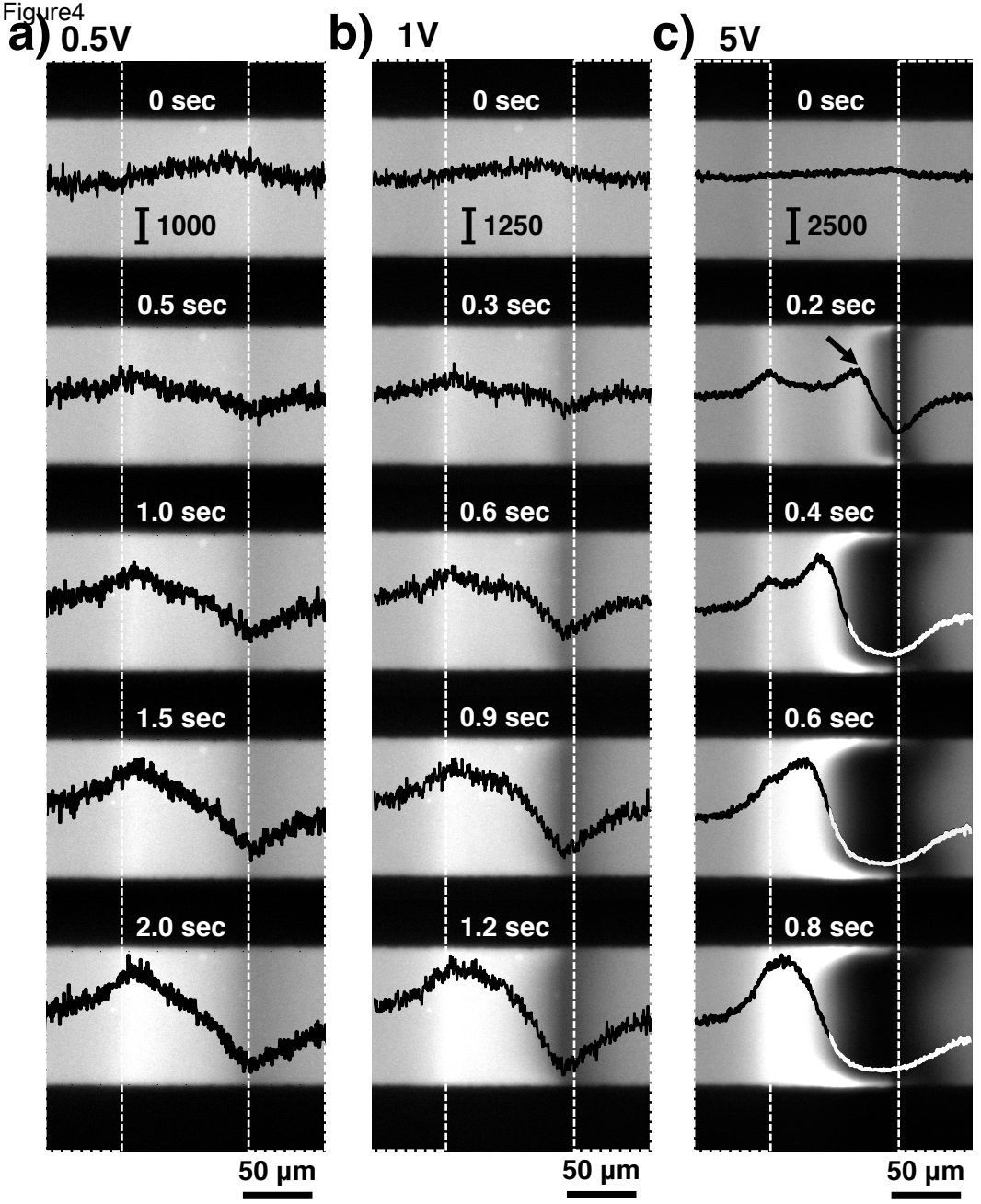

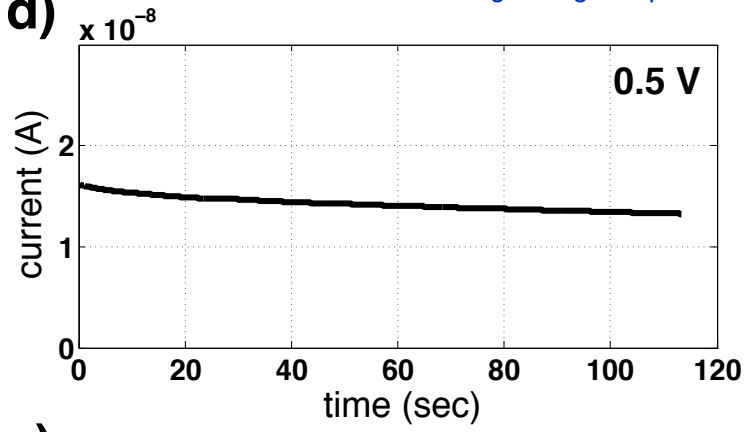

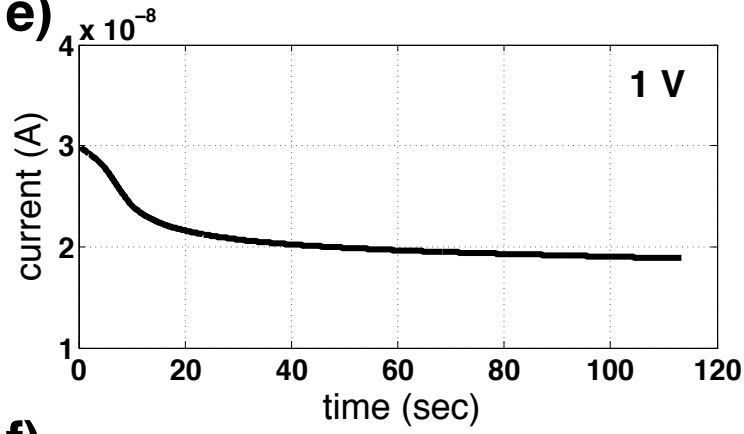

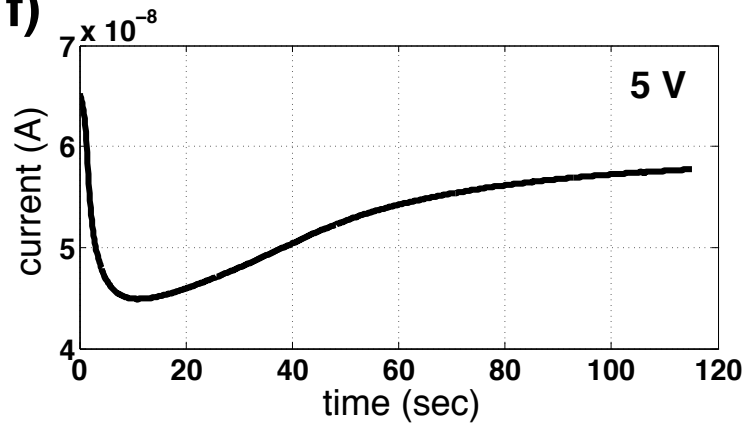

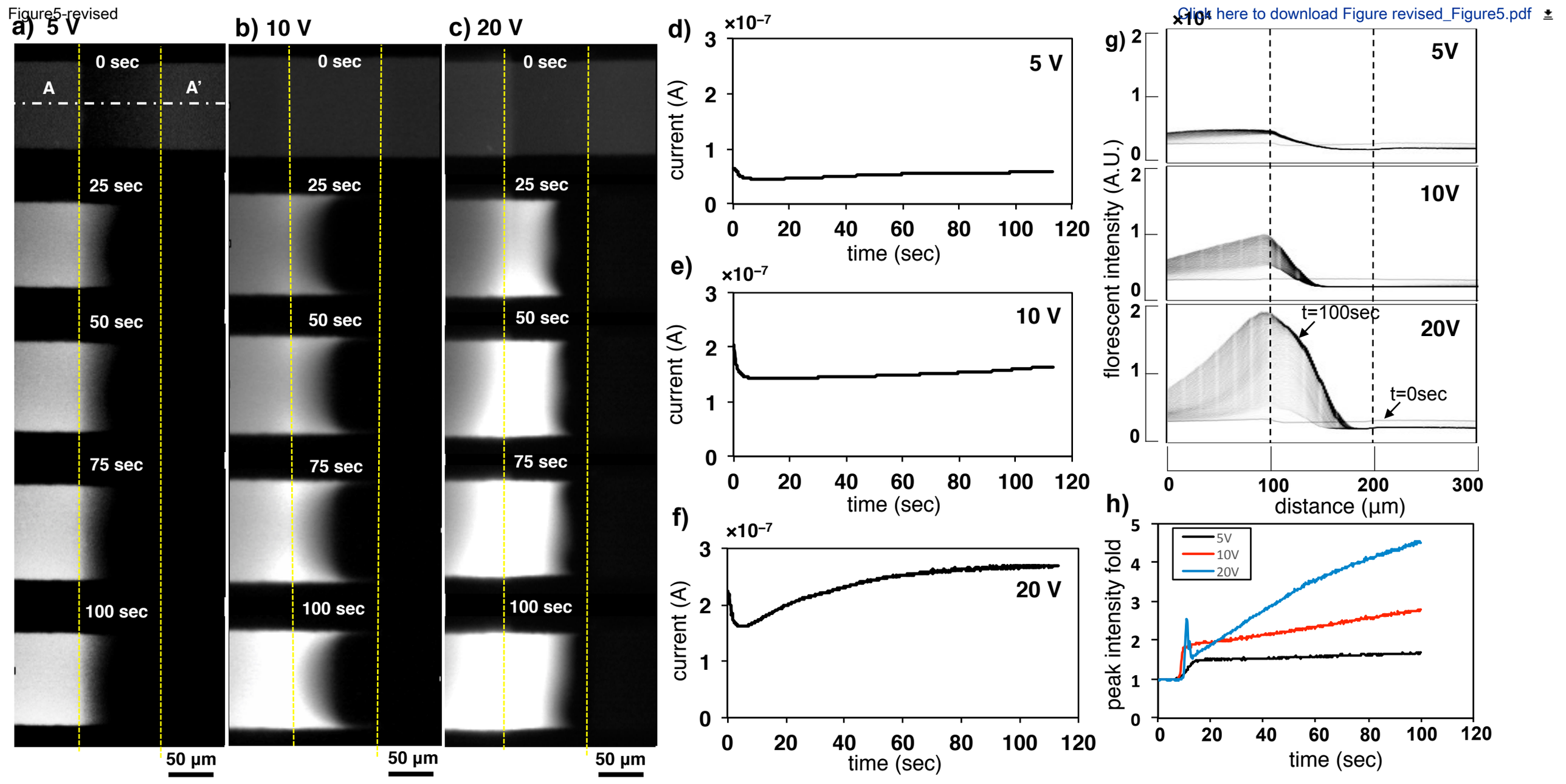

Figure6-revised

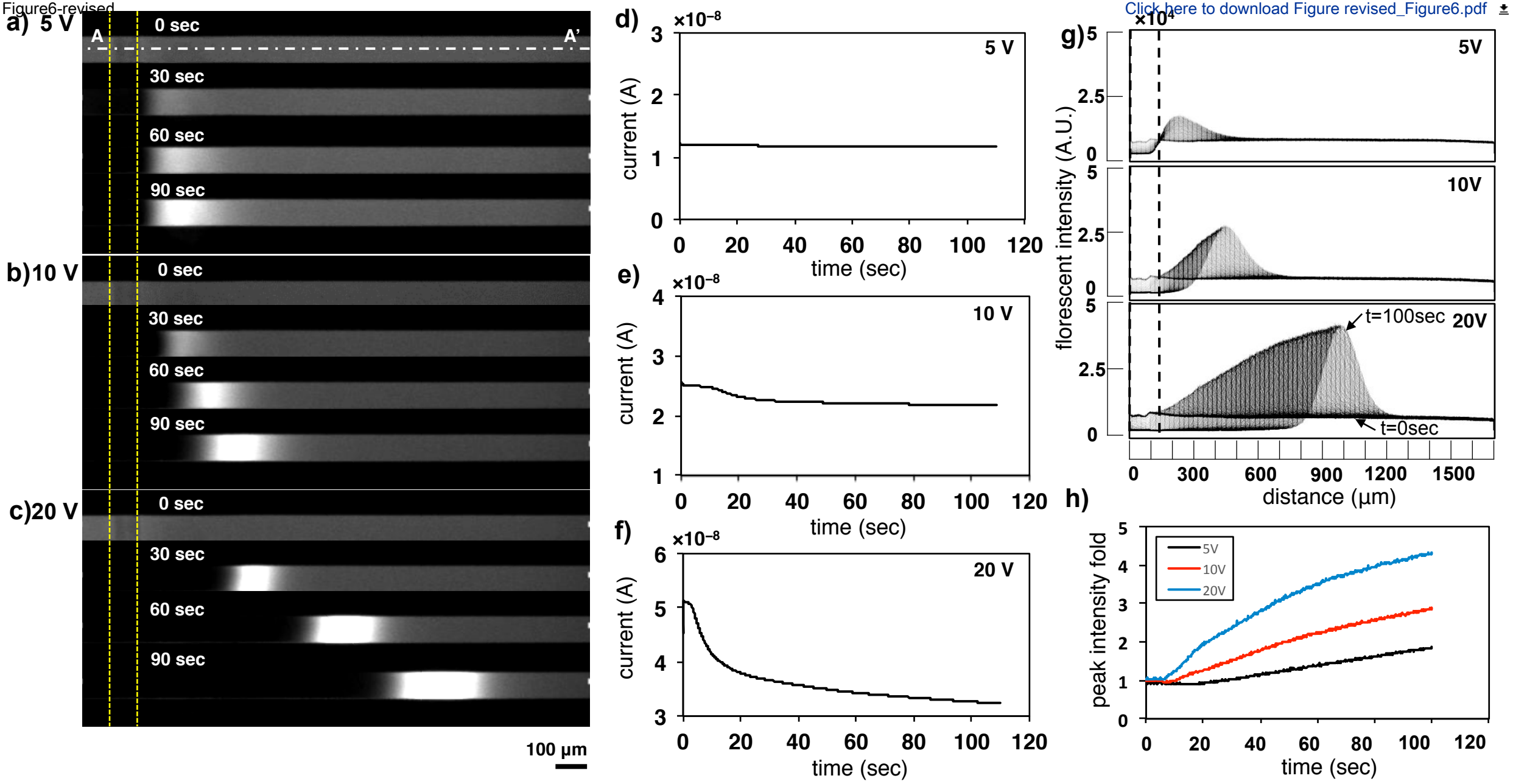

Figure7

Click here to download Figure Figure7.pdf

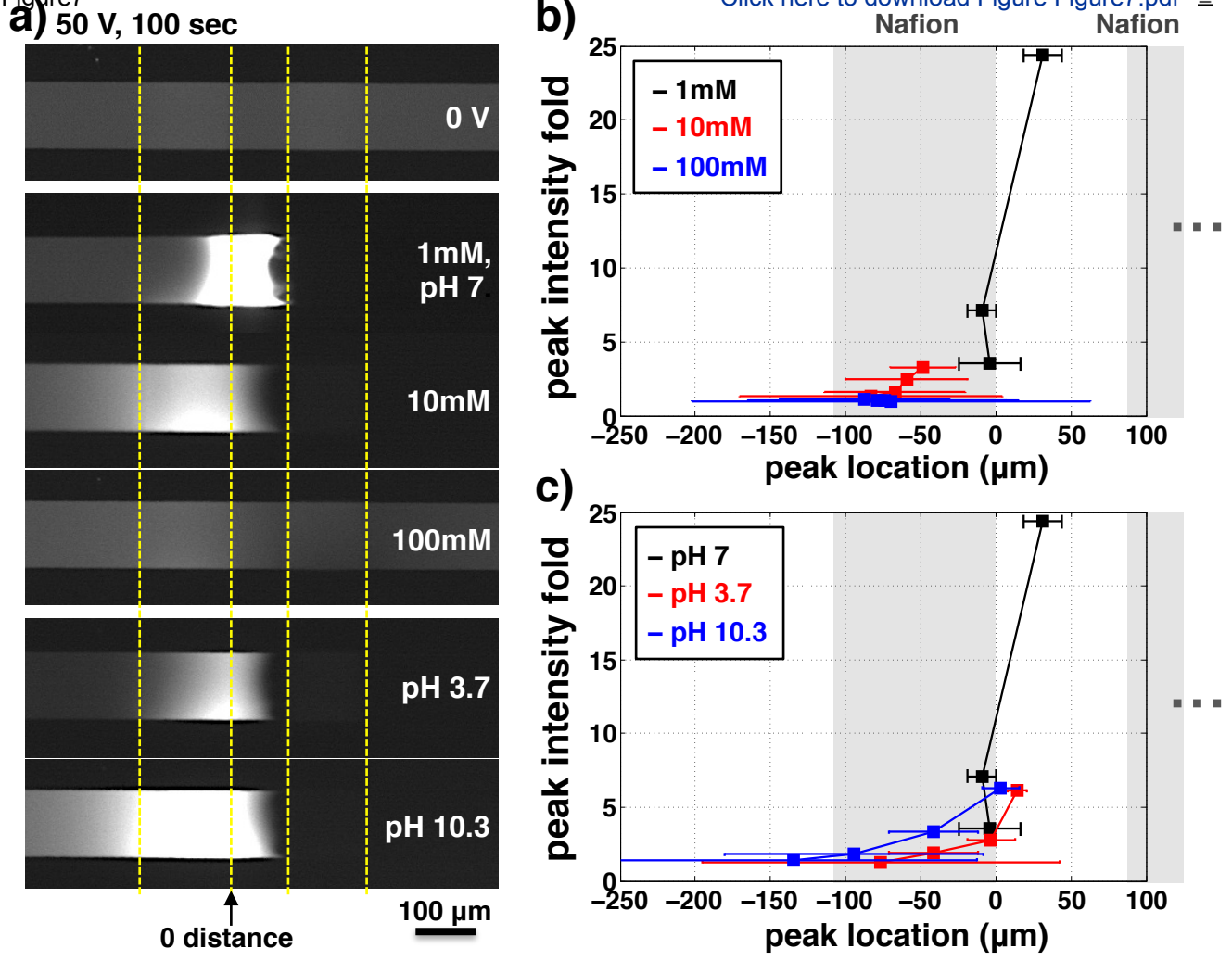

Figure8-revised

Click here to download Figure revised_Figure8.pdf

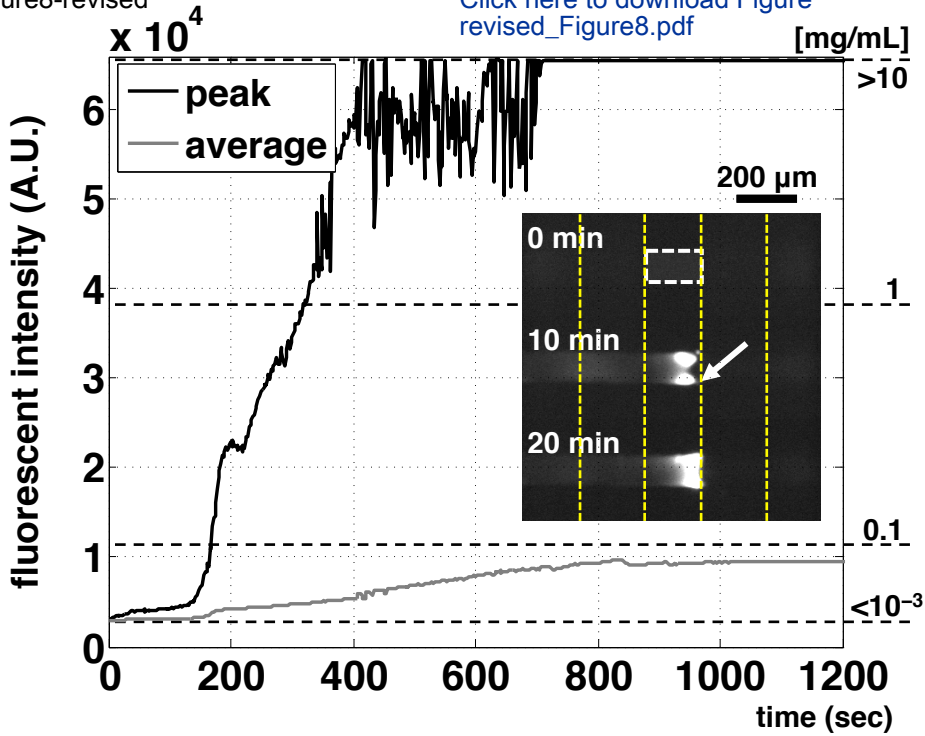

Table of Materials/Equipment

Click here to download Excel Spreadsheet- Table of Materials/Equipment Table of Materials & Equipment.xls

Name of Material/ Equipment	Company	Catalog Number	Comments/Description
Sylgard 184 Silicone Elastomer kit	Dow Corning		
Trichlorosilane	Sigma Aldrich	175552	Highly toxic
Nafion perfluorinated resin, 20 wt%	Sigma Aldrich	527122	
Sodium chloride	Sigma Aldrich	71394	
Potassium chloride	Sigma Aldrich	60121	
Alexa Fluor 488 carboxylic acid, succinii	Invitrogen	A20000	
Isothiocyanate-conjugated albumin	Sigma Aldrich	A9771	
Phosphate buffer saline, 1X	Wengene	LB004-02	
Tween 20	Sigma Aldrich	P1379	
Epifluorescence microscope	Olympus	IX-71	
Charged-coupled device camera	Hamamtsu Co.	ImageEM X2	
Source measurement unit	Keithley Instruments	2635A	
Covance-MP	Femto Science		

1 Alewife Center #200
Cambridge, MA 02140
tel. 617.945.9051
www.jove.com

ARTICLE AND VIDEO LICENSE AGREEMENT

Title of Article: Merging Ion Concentration Polarization between Juxtaposed Ion Exchange Membranes for Blocking Propagation of the Polarization

Author(s): Minyoung Kim, Hyunjoon Rhee, Ji Yoon Kang, Tae Song Kim, Rhokyun Kwak

Merging Ion Concentration Polarization between Juxtaposed Ion Exchange Membranes for Blocking Propagation of the

Item 1 (check one box): The Author elects to have the Materials be made available (as described at http://www.jove.com/publish) via: [V] Standard Access [ ] Open Access

Item 2 (check one box):

[V] The Author is NOT a United States government employee.

[ ] The Author is a United States government employee and the Materials were prepared in the course of his or her duties as a United States government employee.

[ ] The Author is a United States government employee but the Materials were NOT prepared in the course of his or her duties as a United States government employee.

ARTICLE AND VIDEO LICENSE AGREEMENT

1. Defined Terms. As used in this Article and Video License Agreement, the following terms shall have the following meanings: "**Agreement**" means this Article and Video License Agreement; "**Article**" means the article specified on the last page of this Agreement, including any associated materials such as texts, figures, tables, artwork, abstracts, or summaries contained therein; "**Author**" means the author who is a signatory to this Agreement; "**Collective Work**" means a work, such as a periodical issue, anthology or encyclopedia, in which the Materials in their entirety in unmodified form, along with a number of other contributions, constituting separate and independent works in themselves, are assembled into a collective whole; "**CRC License**" means the Creative Commons Attribution-Non Commercial-No Derivs 3.0 Unported Agreement, the terms and conditions of which can be found at: http://creativecommons.org/licenses/by-nc-nd/3.0/legalcode; "**Derivative Work**" means a work based upon the Materials or upon the Materials and other pre-existing works, such as a translation, musical arrangement, dramatization, fictionalization, motion picture version, sound recording, art reproduction, abridgment, condensation, or any other form in which the Materials may be recast, transformed, or adapted; "**Institution**" means the institution, listed on the last page of this Agreement, by which the Author was employed at the time of the creation of the Materials; "**JoVE**" means MyJove Corporation, a Massachusetts corporation and the publisher of *The Journal of Visualized Experiments;* "**Materials**" means the Article and / or the Video; "**Parties**" means the Author and JoVE; "**Video**" means any video(s) made by the Author, alone or in conjunction with any other parties, or by JoVE or its affiliates or agents, individually or in collaboration with the Author or any other parties, incorporating all or any portion of the Article, and in which the Author may or may not appear.

2. Background. The Author, who is the author of the Article, in order to ensure the dissemination and protection of the Article, desires to have the JoVE publish the Article and create and transmit videos based on the Article. In furtherance of such goals, the Parties desire to memorialize in this Agreement the respective rights of each Party in and to the Article and the Video.

3. Grant of Rights in Article. In consideration of JoVE agreeing to publish the Article, the Author hereby grants to JoVE, subject to **Sections 4** and **7** below, the exclusive, royalty-free, perpetual (for the full term of copyright in the Article, including any extensions thereto) license (a) to publish, reproduce, distribute, display and store the Article in all forms, formats and media whether now known or hereafter developed (including without limitation in print, digital and electronic form) throughout the world, (b) to translate the Article into other languages, create adaptations, summaries or extracts of the Article or other Derivative Works (including, without limitation, the Video) or Collective Works based on all or any portion of the Article and exercise all of the rights set forth in (a) above in such translations, adaptations, summaries, extracts, Derivative Works or Collective Works and (c) to license others to do any or all of the above. The foregoing rights may be exercised in all media and formats, whether now known or hereafter devised, and include the right to make such modifications as are technically necessary to exercise the rights in other media and formats. If the "Open Access" box has been checked in **Item 1** above, JoVE and the Author hereby grant to the public all such rights in the Article as provided in, but subject to all limitations and requirements set forth in, the CRC License.

1 Alewife Center #200
Cambridge, MA 02140
tel. 617.945.9051
www.jove.com

4. Retention of Rights in Article. Notwithstanding the exclusive license granted to JoVE in **Section 3** above, the Author shall, with respect to the Article, retain the non-exclusive right to use all or part of the Article for the non-commercial purpose of giving lectures, presentations or teaching classes, and to post a copy of the Article on the Institution's website or the Author's personal website, in each case provided that a link to the Article on the JoVE website is provided and notice of JoVE's copyright in the Article is included. All non-copyright intellectual property rights in and to the Article, such as patent rights, shall remain with the Author.

5. Grant of Rights in Video – Standard Access. This **Section 5** applies if the "Standard Access" box has been checked in **Item 1** above or if no box has been checked in **Item 1** above. In consideration of JoVE agreeing to produce, display or otherwise assist with the Video, the Author hereby acknowledges and agrees that, Subject to **Section 7** below, JoVE is and shall be the sole and exclusive owner of all rights of any nature, including, without limitation, all copyrights, in and to the Video. To the extent that, by law, the Author is deemed, now or at any time in the future, to have any rights of any nature in or to the Video, the Author hereby disclaims all such rights and transfers all such rights to JoVE.

6. Grant of Rights in Video – Open Access. This **Section 6** applies only if the "Open Access" box has been checked in **Item 1** above. In consideration of JoVE agreeing to produce, display or otherwise assist with the Video, the Author hereby grants to JoVE, subject to **Section 7** below, the exclusive, royalty-free, perpetual (for the full term of copyright in the Article, including any extensions thereto) license (a) to publish, reproduce, distribute, display and store the Video in all forms, formats and media whether now known or hereafter developed (including without limitation in print, digital and electronic form) throughout the world, (b) to translate the Video into other languages, create adaptations, summaries or extracts of the Video or other Derivative Works or Collective Works based on all or any portion of the Video and exercise all of the rights set forth in (a) above in such translations, adaptations, summaries, extracts, Derivative Works or Collective Works and (c) to license others to do any or all of the above. The foregoing rights may be exercised in all media and formats, whether now known or hereafter devised, and include the right to make such modifications as are technically necessary to exercise the rights in other media and formats. For any Video to which this Section 6 is applicable, JoVE and the Author hereby grant to the public all such rights in the Video as provided in, but subject to all limitations and requirements set forth in, the CRC License.

7. Government Employees. If the Author is a United States government employee and the Article was prepared in the course of his or her duties as a United States government employee, as indicated in **Item 2** above, and any of the licenses or grants granted by the Author hereunder exceed the scope of the 17 U.S.C. 403, then the rights granted hereunder shall be limited to the maximum rights permitted under such statute. In such case, all provisions contained herein that are not in conflict with such statute shall remain in full force and effect, and all provisions contained herein that do so conflict shall be deemed to be amended so as to provide to JoVE the maximum rights permissible within such statute.

8. Likeness, Privacy, Personality. The Author hereby grants JoVE the right to use the Author's name, voice, likeness, picture, photograph, image, biography and performance in any way, commercial or otherwise, in connection with the Materials and the sale, promotion and distribution thereof. The Author hereby waives any and all rights he or she may have, relating to his or her appearance in the Video or otherwise relating to the Materials, under all applicable privacy, likeness, personality or similar laws.

9. Author Warranties. The Author represents and warrants that the Article is original, that it has not been published, that the copyright interest is owned by the Author (or, if more than one author is listed at the beginning of this Agreement, by such authors collectively) and has not been assigned, licensed, or otherwise transferred to any other party. The Author represents and warrants that the author(s) listed at the top of this Agreement are the only authors of the Materials. If more than one author is listed at the top of this Agreement and if any such author has not entered into a separate Article and Video License Agreement with JoVE relating to the Materials, the Author represents and warrants that the Author has been authorized by each of the other such authors to execute this Agreement on his or her behalf and to bind him or her with respect to the terms of this Agreement as if each of them had been a party hereto as an Author. The Author warrants that the use, reproduction, distribution, public or private performance or display, and/or modification of all or any portion of the Materials does not and will not violate, infringe and/or misappropriate the patent, trademark, intellectual property or other rights of any third party. The Author represents and warrants that it has and will continue to comply with all government, institutional and other regulations, including, without limitation all institutional, laboratory, hospital, ethical, human and animal treatment, privacy, and all other rules, regulations, laws, procedures or guidelines, applicable to the Materials, and that all research involving human and animal subjects has been approved by the Author's relevant institutional review board.

10. JoVE Discretion. If the Author requests the assistance of JoVE in producing the Video in the Author's facility, the Author shall ensure that the presence of JoVE employees, agents or independent contractors is in accordance with the relevant regulations of the Author's institution. If more than one author is listed at the beginning of this Agreement, JoVE may, in its sole discretion, elect not take any action with respect to the Article until such time as it has received complete, executed Article and Video License Agreements from each such author. JoVE reserves the right, in its absolute and sole discretion and without giving any reason therefore, to accept or decline any work submitted to JoVE. JoVE and its employees, agents and independent contractors shall have

1 Alewife Center #200
Cambridge, MA 02140
tel. 617.945.9051
www.jove.com

ARTICLE AND VIDEO LICENSE AGREEMENT

full, unfettered access to the facilities of the Author or of the Author's institution as necessary to make the Video, whether actually published or not. JoVE has sole discretion as to the method of making and publishing the Materials, including, without limitation, to all decisions regarding editing, lighting, filming, timing of publication, if any, length, quality, content and the like.

11. Indemnification. The Author agrees to indemnify JoVE and/or its successors and assigns from and against any and all claims, costs, and expenses, including attorney's fees, arising out of any breach of any warranty or other representations contained herein. The Author further agrees to indemnify and hold harmless JoVE from and against any and all claims, costs, and expenses, including attorney's fees, resulting from the breach by the Author of any representation or warranty contained herein or from allegations or instances of violation of intellectual property rights, damage to the Author's or the Author's institution's facilities, fraud, libel, defamation, research, equipment, experiments, property damage, personal injury, violations of institutional, laboratory, hospital, ethical, human and animal treatment, privacy or other rules, regulations, laws, procedures or guidelines, liabilities and other losses or damages related in any way to the submission of work to JoVE, making of videos by JoVE, or publication in *JoVE* or elsewhere by JoVE. The Author shall be responsible for, and shall hold JoVE harmless from, damages caused by lack of sterilization, lack of cleanliness or by contamination due to the making of a video by JoVE its employees, agents or independent contractors. All sterilization, cleanliness or decontamination procedures shall be solely the responsibility of the Author and shall be undertaken at the Author's expense. All indemnifications provided herein shall include JoVE's attorney's fees and costs related to said losses or damages. Such indemnification and holding harmless shall include such losses or damages incurred by, or in connection with, acts or omissions of JoVE, its employees, agents or independent contractors.

12. Fees. To cover the cost incurred for publication, JoVE must receive payment before production and publication the Materials. Payment is due in 21 days of invoice. Should the Materials not be published due to an editorial or production decision, these funds will be returned to the Author. Withdrawal by the Author of any submitted Materials after final peer review approval will result in a US$1,200 fee to cover pre-production expenses incurred by JoVE. If payment is not received by the completion of filming, production and publication of the Materials will be suspended until payment is received.

13. Transfer, Governing Law. This Agreement may be assigned by JoVE and shall inure to the benefits of any of JoVE's successors and assignees. This Agreement shall be governed and construed by the internal laws of the Commonwealth of Massachusetts without giving effect to any conflict of law provision thereunder. This Agreement may be executed in counterparts, each of which shall be deemed an original, but all of which together shall be deemed to me one and the same agreement. A signed copy of this Agreement delivered by facsimile, e-mail or other means of electronic transmission shall be deemed to have the same legal effect as delivery of an original signed copy of this Agreement.

A signed copy of this document must be sent with all new submissions. Only one Agreement required per submission.

CORRESPONDING AUTHOR:

Name:	Rhokyun Kwak
Department:	Center for BioMicrosystems
Institution:	Korea Institute of Science and Technology
Article Title:	Merging Ion Concentration Polarization between Juxtaposed Ion Exchange Membranes for Blocking Propagation of the Polarization
Signature:	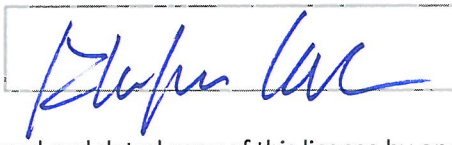 Date: 07/25/2016

Please submit a signed and dated copy of this license by one of the following three methods:

1) Upload a scanned copy of the document as a pfd on the JoVE submission site;
2) Fax the document to +1.866.381.2236;
3) Mail the document to JoVE / Attn: JoVE Editorial / 1 Alewife Center #200 / Cambridge, MA 02139

For questions, please email submissions@jove.com or call +1.617.945.9051

Response to Editorial Comments (JoVE55313R1)

Merging Ion Concentration Polarization between Juxtaposed Ion Exchange Membranes for Blocking Propagation of the Polarization Zone

by Minyoung Kim, Hyunjoon Rhee, Ji Yoon Kang, Tae Song Kim, and Rhokyun Kwak

1. Please proofread the manuscript for numerous minor grammatical and spelling errors (most occur in the procedures section). Examples include, but are not limited to:
-Line 78: "ion depletion near a permselective membrane"
-1.1.2: "Both etching the silicon wafer by deep reactive ion etching and piling the microstructures on the wafer with a photoresist are available." – odd phrasing
-1.2.3: "in order to attach on a glass slide"
-1.3.2. "Then they are attached". Sentences rarely need to begin with "then".
- 2. "Experiment of ICP Preconcentration" should just be ICP Preconcentration, or ICP Preconcentration Experiment.
-2.1.5: "anode on the left reservior"

Response 1: We reviewed the manuscript thoroughly, and corrected grammatical and spelling errors.

2. Detail is needed for step 1.2.1: "place the cup with an uncured PDMS in a vacuum jar" - how much PDMS?

Response 2: 30-40 ml of the uncured PDMS is required to replicate microstructures on a 4-inch silicon wafer. We added this detail in the step 1.2.1.

3. Discussion: Please discuss further applications of the demonstrated technique, and it's advantages over any other similar methods.

Response 3: ICP preconcentrator has been used in the wide range of biomicrofluidic platforms for preconcentrating various bio-agents, amplifying the signals of various assays, and finally detecting the targets such as therapeutic proteins [Ouyang et al., *Anal. Chem.*, 2016, **88**, 9669-9677], peptides [Cheow et al., *Anal. Chem.*, 2014, **86**, 7455-7462], aptamers [Cheow and Han, *Anal. Chem.*, 2011, **83**, 7086-7093], and enzymes [Chen et al., *J. Am. Chem. Soc.* 2011, **133**, 10368-10371]. As one can notice, these previous works targeted fluorescence-labeled biomolecules. This is because that we cannot specify the exact operating condition (e.g. voltage and flow rate) to maintain the preconcentration site, so we need to find the proper condition to preconcentrator targets first.

Starting from the same motivation of our work, Yossifon et al. [*Phys. Rev. E*, 2010, **81**, 046301] suggested the device that can focus the electric field geometrically with nanoslits. Although this method successfully slowed down the propagation of the depletion zone, it could not suppress the propagation perfectly, especially at high voltage and long-time operation for preconcentration applications. Senapati et al. and Slouka et al. accumulated nucleic acids in the ion enrichment zones, and directly used an ion exchange membrane as a

sensor[*Biosens. Bioelectron*. 2014, **60**, 92-100; *Talanta* 2015, **145**, 35-42]. This can bypass the problem of the transient depletion zones, but we should hold the membrane material and the sensing spot on the membrane. Therefore, this platform cannot enjoy the enormous modulations of conventional ICP preconcentrators in materials, geometry, and integrations.

Departing from the previous trials, the merged ICP phenomenon allows us to fix the preconcentrated plugs always at broad range of operating conditions, while maintaining the ICP devices' high flexibility. This indicates that now we can extend the applications of ICP preconcentrators for label-free detection techniques without visualization instruments and tracers. This unique advantage on the spatiotemporal controllability would provide a strong commercial opportunity to integrate the ICP device into generic benchtop platforms, such as for polymerase chain reactions and mass spectrometers.

We added this content in DISCUSSION (Page 9).

4. References: Please include DOI for references, where possible.
5. JoVE reference format requires that the DOIs are included, when available, for all references listed in the article. This is helpful for readers to locate the included references and obtain more information. Please note that often DOIs are not listed with PubMed abstracts and as such, may not be properly included when citing directly from PubMed. In these cases, please manually include DOIs in reference information.

Response 4-5: We added the DOI for the references.

6. If your figures and tables are original and not published previously, please ignore this comment. For figures and tables that have been published before, please include phrases such as "Re-print with permission from (reference#)" or "Modified from.." etc. And please send a copy of the re-print permission for JoVE's record keeping purposes.

Response 6: The phrases regarding reprint permission are added in the figure captions. We also attached a copy of the reprint permission in the package of this revision.

Response to Reviewers' Comments (JoVE55313R1)

Merging Ion Concentration Polarization between Juxtaposed Ion Exchange Membranes for Blocking Propagation of the Polarization Zone

by Minyoung Kim, Hyunjoon Rhee, Ji Yoon Kang, Tae Song Kim, and Rhokyun Kwak

Reviewer #1:

1. The authors have not reviewed the recent advancement in the field of concentration ion polarisation in microfluidics. The fabrication technique presented here has been reported by J Han group at MIT almost 10 years ago. Recent works use paper as microporous material to replace the micro channel and can precent the instability at the concentration/depletion interface: D.T. Phan et al., Sample concentration in a microfluidic paper-based analytical device using ion concentration polarization, Sensors and Actuators B, Vol. 222, No. 1, 2016, pp. 735-740.

Response 1: Thank you for your insightful comment. We agreed that the fabrication technique presented here (i.e. microflow patterning) was developed almost 10 years ago. Various other techniques have been developed to integrate ion selective materials in microfluidics, however, microflow patterning is still the most easy-to-use method. It has been widely used until recently [Cheow et al., *Anal. Chem.*, 2014, **86**, 7455-7462; Cho et al., *Nanoscale*, 2014, **6**, 4620-4626; Choi et al., *RSC Adv.*, 2015, **5**, 66178-66184; Ouyang et al., *Anal. Chem.*, 2016, **88**, 9669-9677].

Our group also has experiences to build ICP preconcentrators in paper-based microfluidic systems [Han et al., *Lap Chip*, 2016, **16**, 2219-2227; Hong et al., *Anal. Chem.*, 2016, **88**, 1682-1687]. As the reviewer 1 addressed, the microporous structures of the paper may prevent the instability by suppressing electroconvective vortices in ion depletion zones [Rubinstein et al., *Phys. Rev. Lett.,* 2008, **101**, 236101; Kwak et al., *Phys. Rev. Lett.,* 2013, **110**, 114501]. However, the sizes of the paper channels are generally about 0.5~5 mm, which is much bigger than the conventional microfluidic channels. This wider paper channel with random fiber networks makes irregular motions of the preconcentrated plugs, instead of the smooth curved shapes in microfluidic channels (Fig. R1). This has been inevitable in paper-based ICP preconcentrators, because the minimum feature size of wax patterning and paper cutting (i.e. fabrication methods to build paper channels) is about few hundred micrometers. We added this explanation in the revised manuscript (Page 9).

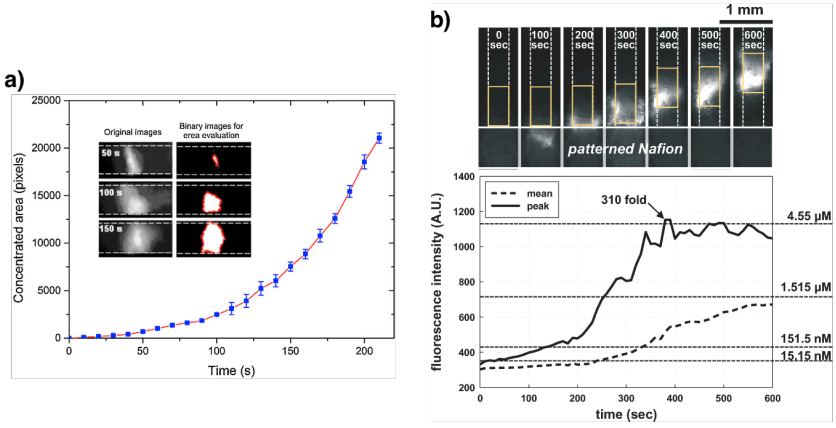

Figure R1. Irregular preconcentrated plugs in paper-based ICP preconcentrators adopted from a) Phan et al. [*Sens. Actuators B* 2016, **222**, 735-740], and b) Han et al. [*Lap Chip*, 2016, **16**, 2219-2227].

Reviewer #3:

1. Usually, the increase of the concentration using ICP is due to the continuous supply of the sample from the reservoir against the ion depletion zone. In the "merged" ICP presented in the manuscript, however, there is no continuous supply of the molecules from the reservoir. It looks like only the molecules confined between the two Nafion membranes get concentrated since there is no continuous supply of molecules from the anodic reservoir. Therefore, the increase is only 4-5 times. However, in Fig. 8, the authors show a 10,000-fold increase which is difficult to understand how. Also, this protein concentration result doesn't correspond to the results presented in Fig. 7 where there is hardly no preconcentration of the dye in 100 mM buffer solution. However, FITC-albumin showed a 100-10,000 fold increase in 1x PBS.

2. in the Discussion section: The first paragraph needs a clarification under which conditions 10,000-fold increase was achieved. In Fig. 7, at 100 mM and pH 3.7, there was hardly any preconcentration achieved. However, in Fig. 8, there was 10,000-fold increase achieved. Why? Any hypothesis?

Response 1-2: As we addressed in the original journal paper [Kwak et al., *Anal. Chem*., 2016, **88**, 988−996], the wall of the PDMS channel is negatively charged, and this generates electro-osmotic flow (EOF) between two Nafion membranes under an electric field (Fig. 2a; i). The EOF delivers targets toward the interface of the depletion and enrichment zones continuously, and its speed is proportional to the applied voltage. As a result, targets are delivered faster at high voltage, resulting faster preconcentration (Fig.5 in the manuscript and Fig. R2). We added these detail descriptions in the caption of Fig. 5 (Page 7).

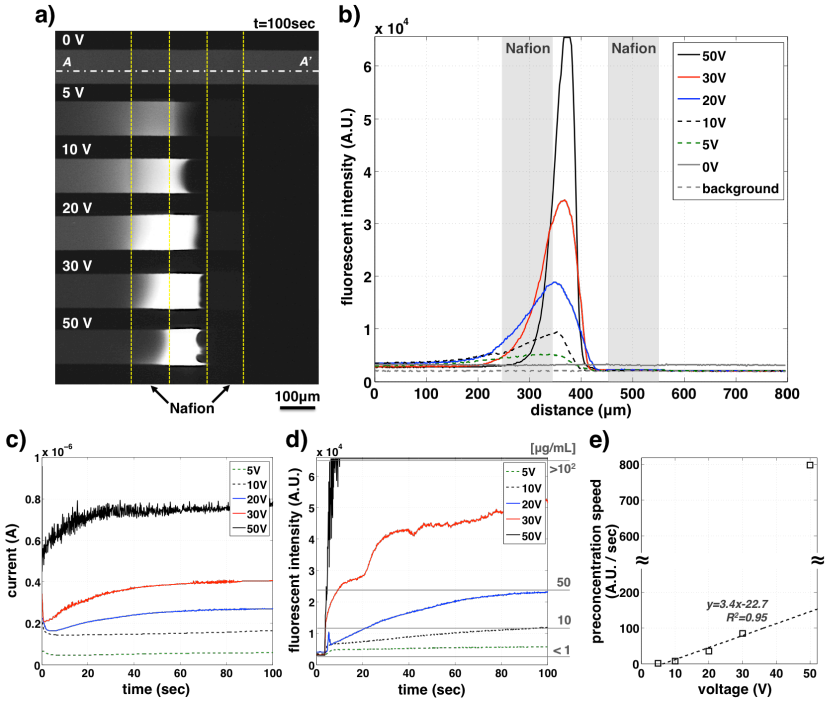

Figure R2. Spatiotemporally defined preconcentration in various operating voltages (5-50V). **a)** Fluorescent images after 100 sec operation, and **b)** fluorescent intensity profiles along *A-A*'. Yellow dotted boxes indicate the location of Nafions. **c)** In these tests, currents are also fully recovered the initial values. **d)** The peak fluorescent intensities are traced during 100 sec with the reference lines, which indicate the actual concentration of fluorescent dyes (1-100 μg/mL of Alexa Fluor 488 in 1mM KCl solution). e) In addition, preconcentration speeds are calculated from the linear regime of the peak intensity-time curves in (d). Under 30V, the preconcentration speed is linearly proportional to the applied voltage (the dotted line is the linear fitting curve), while the speed is much faster at 50V. This figure and contents are adopted from Kwak et al. [*Anal. Chem*., 2016, **88**, 988−996].

Again, we're sorry to drop important information from the original paper [Kwak et al., *Anal. Chem.*, 2016 **88**, 988−996]. As the reviewer 3 addressed, the preconcentration was hardly achieved in higher ionic strength (Fig. 7). Therefore, to facilitate the preconcentration of FITC-albumin in 1x phosphate buffer saline solution, we doubled the width of the Nafion pattern (200 μm) and used a narrower PDMS channel (width: 50 μm). In this way, ICP phenomenon can be enhanced by broadening the ions pathway but by reducing the absolute amount of ions in the channel. We added these detail descriptions in the caption of Fig. 8 (Page 8).

3. A discussion about the effect of the distance between two Nafion membrane is missing in the discussion section. If you increase the distance between two Nafion membranes, can you expect a higher concentration factor since more molecules trapped in between can be preconcentrated? Would the location of the spatiotemporally predefined region be also the same in front of the enrichment zone?

Response 3: As mentioned in the previous response, target molecules can be delivered by EOF, and then the faster EOF at the higher electric field accelerates the preconcentration speed. Therefore, if we increase the distance between two Nafion membranes d, the electric field E decreases under the same applied voltage V ($E=V/d$), resulting the decrease of the preconcentration speed (Fig.R3). We added this discussion in Page 8.

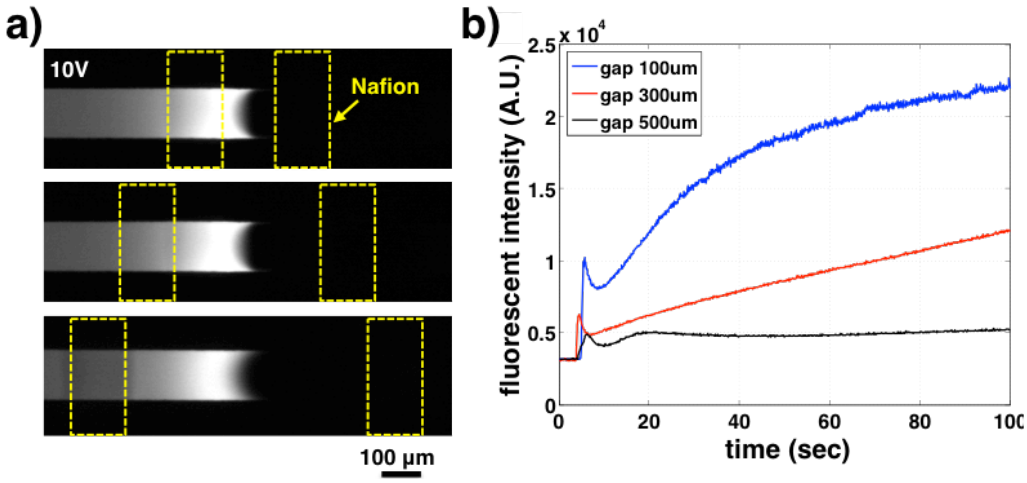

Figure R3. a) Merged ICP preconcentration with various inter-Nafion distances (100, 300, and 500 μm) under 10 V. Yellow boxes indicate the location of the patterned Nafions. b) The peak fluorescent intensities at the applied voltage 10V. The preconcentration plugs are always between the Nafions. However, longer inter-Nafion distances induce weaker preconcentration performance. This figure and contents are adopted from the Figure S2 in Kwak et al. [*Anal. Chem.*, 2016, **88**, 988−996].

4. It is claimed that the location of the plug is spatiotemporally predefined using the merged ICP. What is the longest preconcentration time tested using the merged ICP device? 20 min. are not really a long time for preconcentration. Even using the conventional ICP, a more or less stable plug at the same location can be achieved for ~20 min.

Response 4: Thank you for your valuable comment. Indeed, the longest preconcentration time in our experiments with the merged ICP platform is 20 min (Fig.8). In the FITC-albumin test, we decided that 20 min operation was enough because we achieved 10,000-fold already, and the general operating time in previous works also around few ten minutes [Cheow et al., *Anal. Chem.*, 2014, **86**, 7455-7462; Ouyang et al., *Anal. Chem.*, 2016, **88**, 9669-9677].

We agreed that our experiments could not cover the cases with longer operating times, and addressed this limitation in in the caption of Fig. 8 (Page 8).

5. on page 5, under 1.3.4): Should the PDMS mold be detached right after filling the Nafion resin in the channel? Or is it better to wait a little bit in order to minimize the loss of Nafion stuck on the PDMS surface?

Response 5: In our experiment, the PDMS mold was detached right after filling the Nafion resin. We recommend the detachment time within one minute after filling the resin, but it is not necessary. If we detach the mold few minutes later, we may obtain the thicker Nafion patterns, but the pattern would has a concaved shape; the thickest point would occur at the edge of the pattern because of the capillary effect. We added this content in the Protocol 1.3.4.

6. in the figure caption of Fig. 2: Why is there no increase of the ion concentration in the conventional platform without the ion depletion zone? Is it because there is not enough EOF generated in the channel since the Nafion is grounded and not the right outlet that is floating? What if the right outlet is grounded like the membrane? Would there be a concentration increase in front of the Nafion membrane in conventional ICP? In Fig. 6a, however, there is an increase of the concentration in the form of a plug using the conventional ICP platform. The statement seems to be contradictory. Please clarify this.

Response 6: We addressed that there is no increase of the "ion" concentration in the conventional platform without the ion "enrichment" zone. In this platform, one Nafion pattern rejects ions in the channel, generating only ion depletion zone where ion concentration drops. In this situation, there is no source of ions, so no increase of the ion concentration occurs. This is also directly observed in previous works [Kim et al., *Nanoscale*, 2012, **4**, 7406-7410] (Fig.R4). Also, in Fig. 6a, ion concentration did not increased even the fluorescent dyes were preconcentrated. It is noted that the concentration of a fluorescent dye (and target biomolecules) is not representing the concentration of ions.

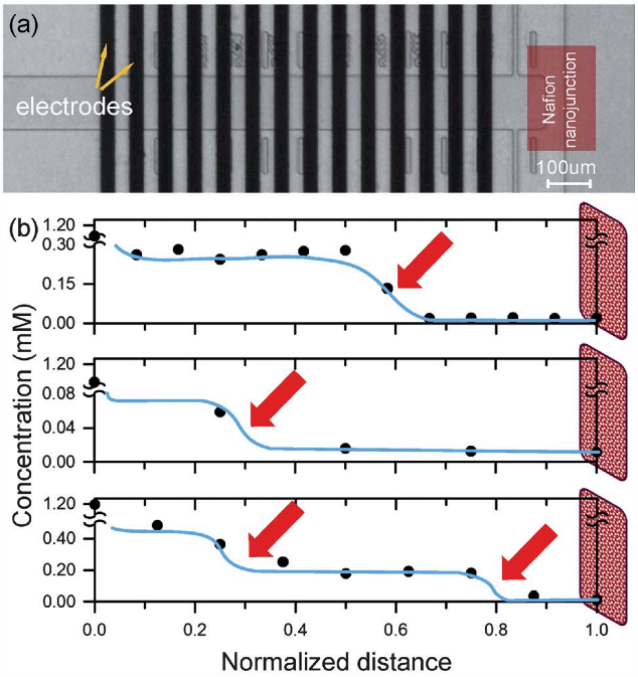

Figure R4. (a) Straight and single micro–nano–microchannel device with microelectrode pairs (black bars) for conductivity measurement experiments. (b) Conductivity drops as a function of normalized distance between ICP interface and Nafion membranes. The y-axes have a break since the concentration steeply decreased right inside ICP layer. The three measurements have different points (denoted by arrows) where the stepwise changes of the electrolyte concentration occurred with multiple vortices in the ion depletion zone. This figure and contents are adopted from Kim et al. [*Nanoscale*, 2012, **4**, 7406-7410].

7. in the figure caption of Fig. 5: why is the depletion shock only observed when the second Nafion membrane is present? A reference would be great if one would like to know more about this depletion shock.

Response 7: Thank you for your valuable comment. We believe that there would be a similar depletion shock in the conventional platform, but it would not make the spike in the peak intensity curves (Fig.5h and Fig.6h).

At high voltage, the flat depletion zone is developed in a moment, and propagates as the ions are rejected through the ion selective membrane continuously. The propagation of the flat depletion zone is reminiscent of the shock propagation, so Mani et al. called this dynamics as the deionization (or depletion) shock [Mani et al., *Phys. Rev. E*, 2011, **84**, 061504].

According to our observations, the fluorescent dyes were accumulated on the shock boundary as it pushes the dyes (Fig.4c). In the conventional platform, this initial accumulation was not identified in the peak intensity curves (Fig.6h); because the fluorescent intensity was keep increasing as the dyes was preconcentrated. However, in the new platform with two Nafion patterns, the initial accumulation was somewhat dispersed when the depletion shock met the ion enrichment zone. As can be seen in Fig.4, the width of the peak at 0.8 sec was wider than that at 0.4 sec. This is probably because the left side of the left Nafion pattern (Fig. 2a) was electrically floated, and the accumulated dyes could spread out. Indeed, in Fig.5g, the slope of the dye concentration was steeper on the right side of the intensity peak that on the left side. We added this content in the caption of Fig. 5-6 (Page 7).

8. in Fig. 6: the ticks on the x- and y-axis are missing in d), e), f). (see Fig. 5d, e, f)

Response 8: We added the ticks on the axis in the revised manuscript.

9. in Fig. 7: why are the yellow dotted boxes are used here while in all other figures, just the dotted lines are used? Use the dotted lines to indicate the Nafion membrane in order to be consistent. What is "0 distance"? In the figure caption of Fig. 7, it says that 10,20, 50 and 100 V were used to map the location of peak intensity. Are the graphs in Fig. 7b) and 7c) based on the results at 50V?

Response 9: Thank you for your specific comment. We changed the word “dotted boxes” to “dotted lines” in Fig. 7. The 0 distance in Fig. 7a represents the origin of the x-axis in Fig. 7b-c, which is on the right edge of the left Nafion membrane.

Next, the data in Fig. 7b-c shows the peak intensity locations and folds under four different voltages (10, 20, 50, and 100 V). For one case (6 cases: 1, 10, 100 mM and/or pH 3.7, 7, and 10), there were four data points corresponding to the four voltage conditions. At higher voltage, we have higher peak intensify fold in all cases. We revised the caption of Fig. 7 for more clear description (Page 7).

10. in Fig. 8: the unit for x-axis [sec.] is missing. Please indicate the location of the Nafion membranes using yellow dotted lines.

Response 10: We added the unit for x-axis, time (sec), and indicated the location of the Nafion membranes with yellow dotted lines.

11. Violent vortices -> strong vortices

Response 11: We changed the word in the revised manuscript.

12. Can you please add a short discussion about how this technique can be applied to enhance the detection sensitivity of a biosensor immobilized with capture molecules in the Discussion section? Plasma bonding of the PDMS chip with a glass slide will compromise the immobilized capture molecules.

Response 12: Thank you for the insightful comment. Indeed, plasma bonding can compromise immobilized capture molecules. Therefore, various protocols and devices have been developed to immobilize molecules after microfluidic channels are built through plasma bonding. There are three representative methods: i) adding target molecules and capture molecules together, and preconcentrating both of them together [Sarkar et al., *Lab Chip*, 2011, **11**, 2569-2576], ii) loading microbeads which holds immobilized molecules [Cheow et al., *Anal. Chem*., 2010, **82**, 3383-3388], and iii) building one bifurcated channel to immobilize capture molecules near the Nafion membrane while the main channel is closed by a value [Liu et al., *Lab Chip*, 2010, **10**, 1485-1490]. We added this discussion in Page 9.